(4) Cemel, A.; Fort, T., Jr.; Lando, J. B. *J. Polym. Sci.* **1972**, *A-1/10*, 2061.
(5) Tieke, B.; Weiss, K. *J. Colloid Interface Sci.* **1984**, *101*, 129.
(6) Laschewsky, A.; Ringsdorf, H.; Schmidt, G. *Thin Solid Films* **1985**, *134*, 153.
(7) Tieke, B. *Adv. Polymer Sci.* **1985**, *71*, 79.
(8) Bader, H.; Dorn, K.; Hupfer, B.; Ringsdorf, H. *Adv. Polym. Sci.* **1985**, *64*, 1.
(9) Schupp, H.; Hupfer, B.; van Wagenen, R. A.; Andrade, J. D.; Ringsdorf, H. *Colloid Polym. Sci.* **1982**, *260*, 262.
(10) Fukuda, K.; Shibasaki, Y.; Nakahara, H. *Thin Solid Films* **1985**, *133*, 39.
(11) Barraud, A.; Rosilio, C.; Ruaudel-Teixier, A. *Polym. Prepr. (Am. Chem. Soc., Div. Polym. Chem.)* **1978**, *19* (2), 179.
(12) Ringsdorf, H.; Schupp, H. *J. Macromol. Sci. Chem.* **1981**, *A15*, 1015.
(13) Piancatelli, G.; Scettri, A.; d'Auria, M. *Synthesis* **1982**, 245.
(14) Albrecht, O. *Thin Solid Films* **1983**, *99*, 227.
(15) Buecher, H.; Elsner, O. V.; Moebius, D.; Tillmann, P.; Wiegand, J. *Z. Phys. Chem. NF* **1969**, *65*, 152.
(16) Gerner, J. Dissertation, Mainz, 1983.
(17) Tyminski, P. N.; Ponticello, I. S.; O'Brien, D. F. *J. Am. Chem. Soc.* **1987**, *109*, 6541.
(18) Green, B. S.; Lahav, M.; Schmidt, G. M. J. *J. Chem. Soc. B* **1971**, 1552.
(19) Kern, W.; Willersinn, H. *Angew. Chem.* **1955**, *67*, 573.
(20) Naegele, D.; Lando, J. B.; Ringsdorf, H. *Macromolecules* **1977**, *10*, 1339.
(21) Enkelmann, V.; Lando, J. B. *J. Polym. Sci., Polym. Chem. Ed.* **1977**, *15*, 1843.
(22) (a) Albrecht, O.; Laschewsky, A.; Ringsdorf, H. *Macromolecules* **1984**, *17*, 937. (b) Albrecht, O.; Laschewsky, A.; Ringsdorf, H. *J. Membrane Sci.* **1985**, *22*, 187.
(23) Fischer, A.; Sackmann, E. *Nature (London)* **1985**, *313*, 299.

Hydrogen-Bonded Highly Regular Strictly Alternating Aliphatic–Aromatic Liquid-Crystalline Poly(ester amides)

Shaul M. Aharoni

Engineered Materials Sector Laboratories, Allied-Signal Corporation, Morristown, New Jersey 07960. *Received December 18, 1987*

ABSTRACT: Forty-seven highly regular strictly alternating poly(ester amides) typified by each aromatic ring being bracketed by several methylene groups were prepared and studied. It was found that when the methylene sequences were sufficiently long, the poly(ester amides) exhibited multiple reproducible first-order transitions upon heating, which did not all reappear upon cooling. Many of the polymers with long alkylene groups grew ordered batonnet-like structures upon cooling from the isotropic melt, but not upon heating. The ordered structures grew upon cooling at temperatures far higher than the uppermost major endotherm in the heating cycle. A combination of DSC and hot-stage cross-polarized light microscopy revealed, upon heating, broad temperature intervals where spontaneous flow and intense or dull birefringence coexisted. Variable-temperature WAXD patterns coupled with X-ray scans on quick-quenched and on oriented samples revealed that in the flowing birefringent polymer upon heating, as well as the "batonnet" interval upon cooling, these poly(ester amides) are probably present in a smectic C liquid-crystalline form. The structure of these polymers, even in the mesomorphic phase, is dominated by H-bonds between amide groups in adjacent chains. Forty-one additional polymers were prepared in which the distances between amide pairs and ester pairs were randomized, the placement of ester and amide was irregular, or the ester group was replaced by either ether or amide groups. All these, as well as eight low molecular weight ester–amide model compounds, failed to show liquid crystallinity. Mesomorphicity appears to be limited to highly regular, strictly alternating aromatic–aliphatic poly(ester amides) in which the methylene sequences are neither too short nor too long and where interchain H-bonds hold the structure together.

Introduction

Polymeric liquid crystals (PLC) are categorized in two major groups: one is endowed with backbone, or main-chain, mesomorphicity and the other exhibits liquid crystallinity due to the nature of its side groups. In this paper only main-chain polymeric liquid crystals (MCPLC) will be considered. The onset of liquid-crystalline behavior of MCPLC may occur in the bulk due to changes in temperature, in which case it is termed thermotropic, or in solution as a result of changes in concentration, upon which it is called lyotropic. The MCPLC are divisible into three major subgroups according to the nature of the mesogenic groups and the interactions giving rise to mesomorphic behavior.

The first subgroup consists of rigid or semirigid worm-like macromolecules having rather large persistence length, q, and the same average rigidity all along the chain. This rigidity may arise from the backbone being aromatic with the rings connected in the para position by groups such as amides, esters, *trans*-vinylene, azo, azoxy, and azomethines, to render them rectilinear or colinear. Among such polymers one finds the lyotropic poly(*p*-benzamide),[1] poly(*p*-phenyleneterephthalamide),[1] and poly(*p*-benzanilide–terephthalamide)[2] and the thermotropic aromatic polyesters prepared from 4-hydroxybenzoic acid and 2-hydroxy-6-naphthoic acid[3] and from terephthalic acid, hydroquinone and 4,4′-biphenol.[3] Because of their rigidity these polymeric chains pack more or less in parallel bundles in space, and because of their polydispersity their liquid crystallinity is nematic in nature. Another kind of highly rigid macromolecule with very large q is the polyisocyanate family.[4] Here we have a highly rigid and extended backbone encased in substantially flexible and mobile side chains. When these are aliphatic or certain aralkyl side chains of appropriate length, the polyisocyanates exhibit both lyotropic and thermotropic liquid crystallinity.[5] In this case the main-chain extension and rigidity are mostly due to the cis–trans configuration of the adjoining amide bonds along the chain.[6,7] A third family of liquid-crystalline polymers is that of the cellulose derivatives.[8] These are mostly lyotropic even though some thermotropic cellulosics were reported in the literature. Depending on the nature and amount of substitution, the cellulose derivatives are soluble and exhibit liquid crys-

0024-9297/88/2221-1941$01.50/0

tallinity in aqueous systems, as in the case of (hydroxypropyl)cellulose, or in nonaqueous solvents, as in the case of cellulose acetate.[9,10] Reflecting the lower chain rigidity of the derivatized cellulose, the solution concentrations at which lyotropic liquid crystallinity becomes evident are far higher than those of the aromatic polyamides.[7] It is important to recognize that in the case of the aromatic polyamides and the derivatized cellulose containing hydrogen bonds (H-bonds), the dissolution and subsequent appearance of lyotropic liquid crystallinity take place in solvents that break the interchain H-bonds and replace them by polymer–solvent H-bonds. When these bonds are replaced by polymer–polymer interchain H-bonds, liquid crystallinity ceases to exist and the polymer precipitates out in a crystalline, semicrystalline, or amorphous state. This phase change is utilized in spinning from the mesomorphic solution highly oriented fibers of polymers such as poly(*p*-phenyleneterephthalamide). A similar phase change occurs during the spinning of thermotropic polyesters into highly anisotropic fibers, except that no H-bonds are involved and no solvent is removed.

The second subgroup of MCPLC is characterized by chains consisting of rodlike mesogenic segments connected by flexible spacers. To attain liquid crystallinity, the axial ratio, x, of the rodlike segments must be not smaller than about 3.[11,12] The flexible spacers along the chain must be sufficiently long to allow for complete, or very large, positional and directional independence of each rodlike segment from its neighbors along the chain. Too short spacers hinder the onset of mesomorphic behavior.[3,13] The necessary axial ratio of the mesogenic segments is usually obtained by the segments comprising at least two para-substituted aromatic rings connected directly or through a substantially rigid group such as amide or ester. Often, the ends of the rigid segment contain additional para-positioned rigid moieties or rings. Other structures simulating the rigid nature of the aromatic rings or connecting groups are also employed occasionally. The important structural feature of the rodlike segments is their axial ratio which calls for the presence of several rigid rings per segment and the absence of hydrogen bonds in the system. Because of their uniform length, it is common for rodlike segments belonging to the same or different chains to pack together in reasonably organized stacks or layers. This layered structure results in smectic liquid crystallinity, with further subdivision arising from the organization of the rods in each layer and their tilt relative to the layer plane. Occasional nematic liquid crystallinity is observed among polymers belonging to this subgroup. Importantly, the mesomorphicity of this subgroup is generally thermotropic. None of the literature references describing this subgroup indicates the presence of intermolecular H-bonding. In fact, it is stated, and then rebuked, that "hydrogen-bonded structures do not form liquid crystals".[14]

The third subgroup of MCPLC comprises biopolymers and biomimetic polymers. Their characteristic feature is an aliphatic main chain twisted in one or another helical form and the helix rendered rigid by intramolecular H-bonds. These hydrogen bonds most often point in the general direction of the helical axis. In almost all cases these MCPLC are lyotropic. Depending on the nature and optical activity of the polymer, the liquid crystallinity may be nematic, smectic, or cholesteric or may change from one another with changes in temperature or concentration.

In this paper the synthesis and initial characterization of a new family of alternating poly(ester amides) will be described. These polymers are substantially aliphatic, their aromatic rings are well separated by strictly alternating alkylene groups, and their bulk is dominated by intermolecular H-bonds more or less perpendicular to the main-chain direction. Employing several conventional techniques, it will be shown that many of the poly(ester amides) exhibit thermotropic polymorphism and mesomorphicity. We know of no other synthetic liquid-crystalline polymer in which the above three structural features coexist. These features are fundamentally different from the characteristic features of the presently known MCPLC described above. In fact, we know of no synthetic MCPLC whose mesomorphicity is dependent on intermolecular H-bonds directed about normally to the main-chain direction. Even among the thousands of thermotropic low molecular weight monomeric liquid crystals (MLC) presently known, there exist only a handful of intermolecularly H-bonded ones. These are all alkyl derivatives of certain carbohydrates.[14,15]

There are four common procedures used in the study of phase transitions of thermotropic polymers and the nature of these phases.[16] The procedures are (1) differential scanning calorimetry (DSC) scans, easily and reliably indicating the temperatures at which phase or mesophase transitions take place; (2) studies of textures observable during microscopic investigation of liquid crystals (using cross-polarized light); (3) studies of the structures of various types of liquid crystals by means of X-ray diffraction patterns; and (4) miscibility relations of liquid-crystalline modifications in binary mixtures. In the case of MLC, the complete miscibility of an unknown with another of known modification is taken to indicate that both are present in an identical modification.[17,18] This miscibility rule was demonstrated to be applicable for PLC, especially in mixtures with MLC analogues,[16] but quite a few exceptions to the rule are reported in the polymer literature.[16,19] In our previous studies on polyisocyanates,[4,20,21] we have found that poly(*n*-octyl isocyanate) (M_w = 108 000) and 1:1 poly(*n*-butyl isocyanate–*p*-anisoyl-2-ethyl isocyanate) (M_w = 161 000) appear not to be miscible across the whole composition range even though both of them are nematic PLC.[21] Because at present there exist no monomeric or low molecular weight liquid-crystalline analogues to our poly(ester amides), because the transition temperatures of these polymers are very much higher than those of the commonly available MLC, and in light of the incompatibility of the polyisocyanate polymers indicated above, no miscibility studies involving the poly(ester amides) were performed. On the other hand, extensive use was made of the three other characterization techniques mentioned above. The general results will be presented below, but specific and detailed DSC and calorimetry studies, X-ray diffraction patterns, infrared, and solid-state NMR spectroscopy results will be presented elsewhere.

It must be borne in mind that the three techniques suffer from inherent or experimental complications and that their interpretation is not always unique. In the case of MCPLC, it is not always possible to differentiate between crystal–crystal, crystal–mesophase, and mesophase–mesophase transitions by studying the DSC traces alone. Input from other techniques, such as microscopy, is needed.[16] It is important to recognize, however, that in heating and cooling cycles the mesophase–isotropic phase and mesophase–mesophase transition temperatures are almost identical, while a marked supercooling is observed for crystal–crystal and crystal–mesophase transitions.[16] High molecular weight MCPLC require an inordinately long time for texture ripening when studied on the hot stage by cross-polarized light microscopy. If the transition

temperatures are high, as is the case with our poly(ester amides), great care must be taken to minimize the polymer degradation during the observations. The combination of high molecular weight and high transition temperatures made it extremely hard to obtain fully ripened textures, and even then only from a few members of the poly(ester amide) family.

The wide-angle X-ray diffraction (WAXD) patterns of crystalline materials are rich in information and allow the determination of the three-dimensional molecular structure of the crystal with rather high precision. The diffraction patterns of liquid crystals suffer from a paucity of information and, in this respect, are much closer to those of liquids than of crystals.[14] As with liquids, the interpretation of WAXD patterns of liquid crystals is, more or less, model-dependent and is never unique.[14]

Bearing the above in mind, all available data from all characterization techniques were considered in the process of determining the mesomorphic nature of the poly(ester amides).

Experimental Section

The monomer 1,3-bis(4-aminobenzoyl)propane

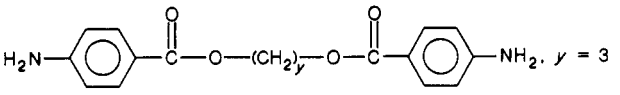

was obtained from Polaroid Corporation (under the trade name of Polacure 740M) and recrystallized prior to use. Its analogues bis(aminobenzoyl)ethane ($y = 2$), bis(aminobenzoyl)butane ($y = 4$), bis(aminobenzoyl)pentane ($y = 5$), and bis(aminobenzoyl)-nonane ($y = 9$) were all prepared in our laboratory in two steps from *p*-nitrobenzoyl chloride and the corresponding diol. In the first step, the dinitro precursor was prepared by a Schotten–Baumann-type reaction in a cold mixture of chlorinated solvent and pyridine. After separation, the dinitro compound was dissolved in *N,N*-dimethylacetamide (DMAc) or in *N,N*-dimethylformamide (DMF) at temperatures from 60 to 120 °C and reduced in high yield to the diamine by high pressure hydrogenation in the presence of Raney nickel. After workup the resulting diamine was of purity sufficient for polymerization. The monomers bis-(aminophenoxy)alkane

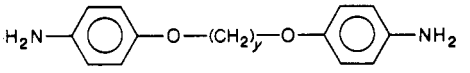

with $y = 3$, 6, and 8, were prepared in our laboratory in two steps from 4-acetamidophenol and linear α,ω-dibromoalkane. In the first step the diether was formed under mild conditions.[22] Then the reaction product was hydrolyzed by using either the procedure of Strzelecki and Van Luyen[22] or that of Bartulin et al.[23] After workup the monomers were sufficiently pure for polymerization. All other monomers and reagents were used as received. All solvents were of reagent grade or better and were used as received, except for light scattering purposes where they were filtered through 220-nm Millipore filters prior to use and again during sample preparation.

Most polymers were prepared from the acids and aromatic amines in the presence of triphenyl phosphite (TPP) and pyridine, according to the procedure of Yamazaki et al.[24] following the details described in ref 11 and 25. One polymer was synthesized from sebacoyl chloride and bis(aminobenzoyl)propane by using Schotten–Baumann-type reaction conditions. The solvent DMAc was found to be convenient in this instance. The polymerization was continued for 3 h at 23 °C with the workup similar to the above procedure. An additional polymer was prepared by melt polycondensation following the procedure of Laakso and Reynolds[26] and Manzini et al.,[27] in the presence of catalytic amounts of Zn/Sb ions. Here, 1,5-pentanediol was condensed with the monomer which was previously prepared by the Schotten–Baumann procedure from sebacoyl chloride and ethyl *p*-aminobenzoate. The polycondensation proceeded for 1 h at 240 °C and after the evolution of ethanol subsided, for an additional 3 h at

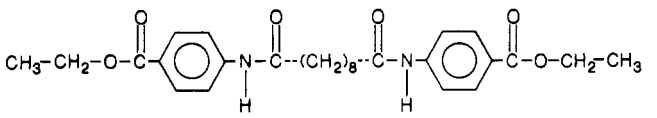

260 °C under high vacuum. A high molecular weight, tough polymer was recovered. Low molecular weight model compounds were prepared by both the Yamazaki and Schotten–Baumann procedures in a fashion similar to the above.

The structure of all polymers and model compounds prepared by us, as well as all the monomers and their precursors, was confirmed by ^{13}C NMR spectra, obtained with a Varian XL-200 Fourier transform NMR spectrometer from about 10% solutions in solvents such as DMAc-d_9, DMF-d_7, and deuteriated chloroform. Infrared (IR) spectra in the 4000–400-cm^{-1} range were obtained from thin films of the polymers either molded at elevated temperatures or cast from DMF solution on KBr windows and subsequently dried and/or annealed thoroughly. The spectra were obtained at 2-cm^{-1} resolution with a Nicolet 170SX FTIR instrument with the specimens placed in dry nitrogen atmposphere. For variable-temperature studies the specimens were sealed in an Accuspec Model 20 heated cell with a controller capable of maintaining temperatures to within ±1 °C. In each variable-temperature study the sample was heated at a rate of about 10 K/min to the desired temperature and allowed to equilibrate for at least 10 min before the scan was started. Additional room temperature IR spectra were obtained at the same resolution with Perkin-Elmer Model 283B and Mattson Cygnus 100 spectrometers.

Dilute solution viscosities were measured at 25 °C on solutions of all the polymers in DMAc containing 5 wt/vol % dry LiCl, using Cannon-Ubbelohde internal dilution glass viscometers with solvent efflux time longer than 100 s. Weight-average molecular weight, M_w, and hydrodynamic radii, R_H, were measured respectively in a low-angle laser light scattering Chromatix KMX-6 instrument and in a Langley-Ford LSA II photon correlation spectrometer. Molecular weight distributions and number-average molecular weight, M_n, were obtained by size-exclusion chromatography, using hot DMF as solvent and a Waters Model 150-C GPC instrument.

Thermal studies were conducted by using a Du Pont Model 9900 differential scanning calorimeter. The heating and cooling rates were generally 10 K/min, but faster and slower rates were used when deemed necessary. The sample sizes were in the range 5–10 mg. The samples were always in a dry nitrogen atmosphere during the thermal scans. Cross-polarized light microscopy studies were conducted with an Olympus BH-2 microscope equipped with a Reichert hot stage or with a Mettler FP-82 hot stage capable of reaching 350 °C and controlled by a Mettler FP-80 central processor. All original magnifications of the micrographs were 100× unless specified otherwise.

Films 0.05–0.5 mm thick were molded in windows of set thickness between poly(tetrafluoroethylene)-coated thin aluminum foils in a Carver laboratory press equipped with controlled temperature platens capable of reaching 320 °C. In many instances polymers were subjected in the press to heat treatments (heating cycle, cooling cycle, heat and cool cycle, anneal, etc.) identical with those in the DSC and microscopy studies. At the end of such a heat treatment, the film was very rapidly quick quenched in an ice/water mixture and then allowed to reach room temperature. Microscopy studies revealed that the morphologies observed in such quick quenched films were essentially identical with those observed in the films at the temperatures from which they were quick quenched. Several poly(ester amides) were molded above their clearing points to produce films 0.25 mm thick. These films were quick quenched and WAXD patterns indicated them to be amorphous. Strips were cut from the films, heated to the point where intense birefringence appeared in them, stretched by hand at this temperature to produce a draw ratio of 3–5, and then rapidly quenched in an ice/water mixture. Highly crystalline strips could not be significantly drawn and tore in the process.

Wide-angle X-ray diffraction (WAXD) patterns were collected at ambient temperature from powdered samples, unoriented molded films, and heat-treated quick-quenched films by using a Philips APD 3600 automated diffractometer operating in parafocus mode and using monochromatized copper Kα radiation. The same procedure was used to obtain the equatorial reflections

from oriented samples. Transmission scans in the same diffractometer were conducted to record the meridional data. Flat plate photographs were obtained from all oriented samples by using an appropriate custom-made X-ray camera. Variable-temperature WAXD patterns were generated from samples having 1–2-mm path length, wrapped in 0.015-mm aluminum foil, and sandwiched between two coated beryllium foils. This assembly was positioned in a Mettler FP-84 hot stage modified for use with X-rays in transmission geometry. The hot plate was mounted on a Huber two-circle goniometer. The data were collected by using nickel-filtered copper Kα radiation and a Xentronic/Nicolet area detector. Heating and cooling rates were 10 K/min. WAXD patterns were collected at each predetermined temperature after the sample was equilibrated there for not less than 5 min. Variable-temperature X-ray scans in the Huber machine and room temperature scans on quick-quenched samples in both the Huber machine and the Philips diffractometer yielded for the corresponding samples essentially identical WAXD patterns. This and the corresponding microscopy observations indicate that both the microscopic textures and the molecular organization existing in the samples at elevated temperatures are retained at ambient temperature by quick quenching in an ice/water mixture.

Mechanical properties of spun and of drawn fibers were measured at room temperature in an Instron instrument by using a constant strain rate of 5 in. min^{-1}.

Results and Discussion

The polymers synthesized in the course of this study will first be presented. Then the results of DSC and microscopy studies will be discussed. With liquid crystallinity defined as multiple endothermic transitions upon heating coexisting with mobile and/or spontaneously flowing birefringent mass, it will be shown that a large number of highly regular strictly alternating poly(ester amides) are liquid crystalline. Many other poly(ester amides) in which the regularity is disrupted by various means and analogous polyamides, polyesters and poly(ether amides) will be shown not to be liquid crystalline. The DSC/microscopy conclusions will then be corroborated by a variety of X-ray studies, and a crude model for the thermotropic mesomorphic poly(ester amides) will be suggested.

(a) Synthesized Polymers. A large family of strictly alternating, highly regular poly(ester amides) of the exact structural formula

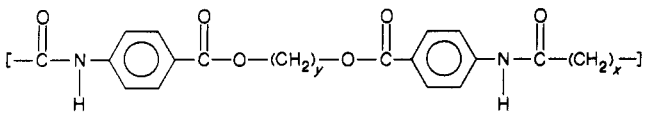

were prepared by the Yamazaki procedure[11,24,25] at moderate temperatures (100–115 °C) from the preformed bis(aminobenzoyls) and aliphatic diacids. They are listed together with their intrinsic viscosities, [η], in Table I. The structure of the poly(ester amides) and strict alternation of the two ester groups and two amide groups along the chain were confirmed by carbon-13 NMR scans of the polymers, of an additional similar poly(ester amide) prepared in the cold by the Schotten–Baumann reaction, and of model compounds prepared at modest temperatures by the Yamazaki procedure and in cold solvent by the Schotten–Baumann method. The high crystallinity and multiple thermal transitions to be described below also indicate highly ordered polymers. The molecular weights of several poly(ester amides) were measured by light scattering and are shown in Table I. Weight-average molecular weights determined by size-exclusion chromatography (SEC) were in excellent agreement with those obtained from light scattering. The ratio M_w/M_n determined by SEC was 1.62 ± 0.02 for all polymers studied. For the sake of comparison, many other poly(ester amides) containing different structural features and a variety of monomer mixtures were similarly prepared and are tabulated in Tables II and III, respectively. Several poly(ether

Table I
Strictly Alternating Aromatic–Aliphatic Poly(ester amides)[a]

no.	y	x	[η], dL/g	M_w	R_H, Å
1	2	3	0.40		
2	2	4	0.58		
3	2	7	0.87		
4	2	8	0.64		
5	2	14	0.50		
6	3	0	insoluble		
7	3	1	0.26, 0.26	11 500, 10 100	19, 21
8	3	2	0.26	6800	22
9	3	3	0.57, 1.06, 1.66	18 000	33
10	3	4	0.72, 1.42	52 000	44
11	3	5	0.78, 0.77	65 000	57
12	3	6	1.07, 1.21, 1.34	92 000	60
13	3	7	1.38, 1.75, 1.82	137 000	99
14	3	8	1.45, 1.35, 1.86	73 000	95
15	3	10	1.86, 1.09	108 000	97
16	3	11	0.87	37 000	65
17	3	12	1.02	62 000	69
18	3	14	0.65, 0.84, 0.91		
19	3	20	0.70		
20	4	2	0.24		
21	4	3	0.55		
22	4	4	0.73		
23	4	5	0.68		
24	4	6	0.59		
25	4	7	1.33		
26	4	8	1.26		
27	4	10	0.90		
28	4	11	0.72		
29	4	14	0.61		
30	5	3	0.39, 0.72		
31	5	4	0.65		
32	5	5	0.52		
33	5	6	0.57		
34	5	7	0.76		
35	5	8	0.86		
36	5	10	0.47		
37	5	11	0.52		
38	5	12	0.39		
39	5	14	0.60, 0.73		
40	5	20	0.37		
41	9	3	0.64		
42	9	4	0.53		
43	9	7	0.50		
44	9	8	0.60, 0.52		
45	9	11	0.61		
46	9	12	0.58		
47	9	14	0.65		

[a] Many of the poly(ester amides) were prepared in several batches. Intrinsic viscosities recorded above are representative. Underlined values belong to the same batch for which M_w and R_H were determined.

Table II
Poly(ester amide) Analogues from Bis(aminobenzoyl)propane (y = 3)

no.	diacid	[η], dL/g	analogous to
1	*trans,trans*-muconic	0.75	y = 3, x = 4
2	*trans*-1,4-cyclohexadienecarboxylic	0.44	y = 3, x = 4
3	3-methyladipic, racemic	0.90	y = 3, x = 4
4	hydromuconic	0.77	y = 3, x = 4
5	2,6-naphthalene dicarboxylic	0.57	y = 3, x = 4
6	terephthalic	0.83	y = 3, x = 4
7	isophthalic	0.63	y = 3, x = 4
8	3-methylglutaric	0.46	y = 3, x = 3
9	2-methylglutaric	0.41	y = 3, x = 3
10	2,2-dimethylglutaric	0.19	y = 3, x = 3
11	3,3-dimethylglutaric	0.30	y = 3, x = 3
12	diglycolic	0.26	y = 3, x = 3
13	maleic (cis)	0.27	y = 3, x = 2
14	fumaric (trans)	0.52	y = 3, x = 2

Table III
Strictly Alternating Poly(ester amides) with Equimolar Mixtures of Diacids or Bis(aminobenzoyls)

no.	y	x	[η], dL/g	melting point, °C
1	3	3 + 4	0.66	178
2	3	7 + 6	1.79	147
3	3	7 + 8	2.07	152
4	3	3 + 7	0.81	167
5	3	5 + 7	0.84	190
6	3	8 + 4	1.55	172
7	3	8 + 10	1.79	186
8	3 + 4	10	1.12	203
9	2 + 4	10	0.88	233
10	3 + 4	7 + 10	1.11	139
11	2 + 4	7 + 10	0.88	196

Table IV
Strictly Alternating Poly(ether amides)

no.	y	x	[η], dL/g
1	3	3	0.43
2	3	4	0.41
3	3	7	1.10
4	3	8	0.65
5	6	7	0.54
6	8	3	0.49
7	8	4	0.52

amides) (Table IV) and polyamides (Table V) were also prepared for comparison. For brevity, the poly(ester amides) and poly(ether amides) below will be denoted by their y and x values.

In order to check whether the polymerization method affects the nature and strict alternation of the resulting poly(ester amide), two such polymers were prepared by methods other than the Yamazaki procedure. In one case, a poly(ester amide) with $y = 3$, $x = 8$ was synthesized by the Schotten–Baumann method at 23 °C. The resulting polymer, with $[\eta] = 0.71$ dL/g in DMAc/5% LiCl, was found by carbon-13 NMR spectroscopy to be identical with its analogue prepared by the Yamazaki procedure. Furthermore, the WAXD patterns of both polymers, and their thermal behavior and multiple transitions, were essentially identical. In the other case, a poly(ester amide) which is supposed to correspond to $y = 5$, $x = 8$ was prepared at elevated temperatures (240–260 °C) according to the procedure of Laakso and Reynolds.[26] Its intrinsic viscosity was 0.65 dL/g. When studied by DSC, WAXD, and hot-stage cross-polarized light microscopy, the resulting polymer was found to be almost completely amorphous and devoid of the multiple first-order transitions observed in its strictly alternating analogue. The extremely low crystallinity of this polymer reflects randomness along the chain, in contrast with the regularity obtained by the Yamazaki procedure. A low level of crystallinity and a single melting point for as-prepared and annealed samples were indicated by Manzini et al.[27] for a series of melt-polymerized poly(ester amides). It is well-known that during condensation polymerizations carried out in the molten state or in solution at elevated temperatures (200 °C and above), the molecular species are in a state of mobile interchange or equilibrium, with end groups reacting with functional groups in the polymer chain.[28] These interchange reactions include both transesterification and transamidation[29] and are rather rapid at elevated temperatures, especially in the presence of catalysts and when the volatile byproducts are being removed by high vacuum. From the above it becomes obvious that low- and moderate-temperature solution polycondensations using preformed esters proceed under such mild conditions that the ester groups remain intact. This results in high molecular weight, highly crystalline poly(ester amides) containing strictly alternating alkylene groups and pairs of ester and amide groups. Conversely, the high-temperature melt polycondensation disrupts the ester and amide groups and leads to amorphous or low-crystallinity poly(ester amides) in which the placement of these groups is scrambled and the length of the methylene sequences is not strictly alternating. In conclusion, the

Table V
Comparable Polyamides

structure	[η], dL/g	monomers
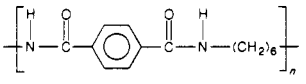	nylon 6T	terephthalic acid + hexamethylenediamine
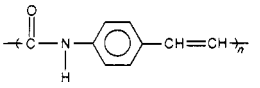	0.85	4-aminocinnamic acid
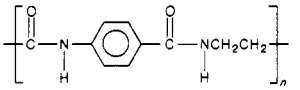	insoluble	*N*-(*p*-aminobenzoyl)β-alanine
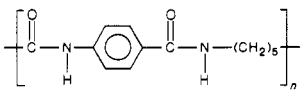	1.38	*N*-(*p*-aminobenzoyl)-6-aminocaproic acid
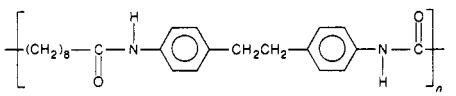	1.18	sebacic acid + ethylenebis(aniline)
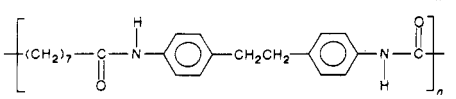	1.22	azelaic acid + ethylenebis(aniline)
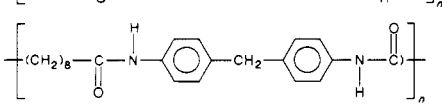	1.95	sebacic acid + methylenebis(aniline)
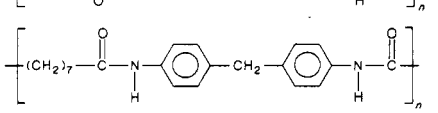	1.45	azelaic acid + methylenebis(aniline)

strict regularity of the poly(ester amides) listed in Table I, together with the fact that each aromatic ring is bracketed by alkylene sequences, stands in contradistinction to other poly(ester amides) reported in the literature. Among these one finds poly(ester amides) prepared by melt polymerization,[26,27] random poly(ester amides) from precursor polyesters,[30] poly(ester amides) with random placement of ester and amide groups between aromatic rings,[31,32] and ordered poly(ester amides) either fully aromatic[33] or containing a substantial fraction of sequences of three or more aromatic rings[34] or with pairs of rings connected by an ester group.[35]

The 14 poly(ester amides) listed in Table II were prepared by the Yamazaki procedure from bis(4-aminobenzoyl)propane (y = 3) and diacids imparting substantially lower chain flexibility or having substituents on the chain. They were all studied by DSC and microscopy. All showed a single melting point, occasioned by some crosslinking of those containing double bonds. None showed mesomorphic behavior. When two diacids or two diaminobenzoyls of different lengths were copolymerized in the same poly(ester amide), no mesomorphicity was ever detected. All polymers so synthesized are listed in Table III. In all instances these polymers showed only one reproducible endotherm in the DSC scans, which was found by microscopy to be a simple melting point. The percent crystallinity as measured by X-ray techniques was surprisingly high, between 30% and 40%. This was unexpected, considering the lack of order in the repeat distances between the ester and amide pairs along the chain and the very low crystallinity of the scrambled poly(ester amides) prepared by melt polycondensation. A replacement of the ester group by ether oxygen, in the poly(ether amides) in Table IV, fully suppressed mesomorphicity, and only normal melting point were observed for these polymers. When the ester groups were replaced by amides and a highly regular aliphatic–aromatic polyamide was obtained, no thermotropic liquid crystallinity was observed. This is true for all the rather high molecular weight polyamides in Table V as well as for the nylons 2T, 3T, 4T, 5T, and 6T, which are known not to be liquid crystalline.[36] When the amide groups are, conversely, replaced by esters, a regular aliphatic–aromatic polyester is obtained. Representative of such polyesters are the poly(alkylene terephthalates). None of these crystalline polyesters exhibits a mesomorphic interphase.[37] Thus, the ability to undergo mesomorphic transitions rests neither with the polyamides nor the polyesters but only with the highly regular strictly alternating aliphatic–aromatic poly(ester amides) in which both the placements of amide and ester groups as well as the distances between them are highly regular, with the added restriction of the appropriate values of y and x.

In addition to the melt polycondensation described above, we checked on the effects of random placement of the amide and ester groups along the chain by preparing two poly(ester amides) where the placements are irregular and dictated by statistics. One random poly(ester amide) was prepared under Schotten–Baumann-type conditions from sebacoyl chloride and p-aminophenol. This should be the random version of y = 8, x = 8. The resulting low molecular weight ([η] = 0.2 dL/g) polymer showed no mesomorphicity. The second poly(ester amide) was prepared under Yamazaki conditions from N-(p-aminobenzoyl)-6-aminocaproic acid, suberic acid, and 1,3-bis(4-aminobenzoyl)propane. This high molecular weight polymer ([η] = 1.72 dL/g), which is the random analogue of the strictly alternating y = 3, x = 6, did not show any liquid-crystalline behavior.

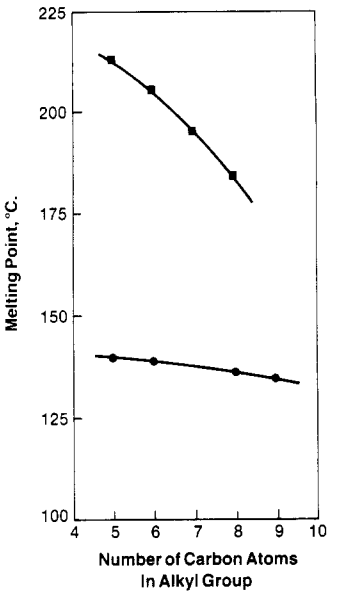

Figure 1. Melting points of model compounds prepared from bis(4-aminobenzoyl)propane and aliphatic acids (●) or p-alkylbenzoic acid (■). Notice the absence of odd–even effects.

In order to check whether the polymeric state is necessary for liquid crystallinity, two series of monomeric model compounds were prepared and studied by DSC and microscopy. One series, prepared from bis(aminobenzoyl)propane and linear aliphatic acids, had the general structure

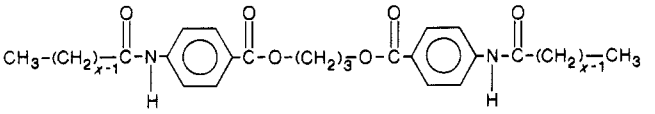

with x = 5, 6, 8, and 9. The other series was prepared with p-alkylbenzoic acid and had the structure

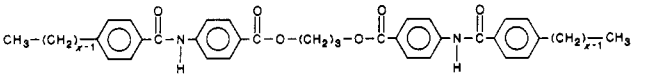

with x = 5, 6, 7, and 8. All model compounds were characterized by NMR and had very narrow DSC melting endotherm. None exhibited liquid crystallinity, and there was no noticeable odd–even effect within each family. A transition map of both series is shown in Figure 1. The above clearly indicates that the thermotropic mesomorphicity is a feature of *polymeric* ester amides and that their monomeric analogues are incapable of exhibiting liquid-crystalline behavior.

(b) DSC and Microscopy Studies. DSC and microscopy studies of highly regular strictly alternating poly(ester amides) will be presented below. A calorimetric study of the mesomorphic poly(ester amides) will be presented elsewhere. The DSC scans of all poly(ester amides) with y = 2, in Table I, exhibited a single reproducible endotherm upon heating. A typical such scan for the poly(ester amide) y = 2, x = 14 is shown in Figure 2. Upon cooling in the DSC instrument, a single crystallization exotherm appeared at substantial supercooling. Hot-stage cross-polarized light microscopy revealed the endothermic transition to be a simple melting point in which the substantially crystalline polymers melt directly into a fully extinguishing isotropic mobile fluid. When pressure was applied to the microscope coverslip below the melting point, T_m, the sample under it showed no signs of yield or flow. On the contrary, they were fully resilient right up to T_m. A transition map of all available members

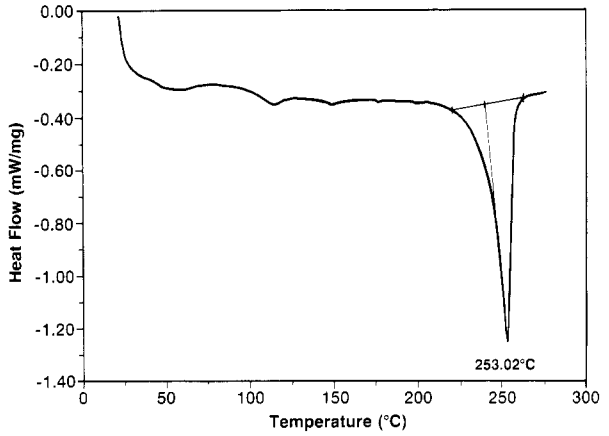

Figure 2. Heating cycle of DSC scan of poly(ester amide) with $y = 2$, $x = 14$.

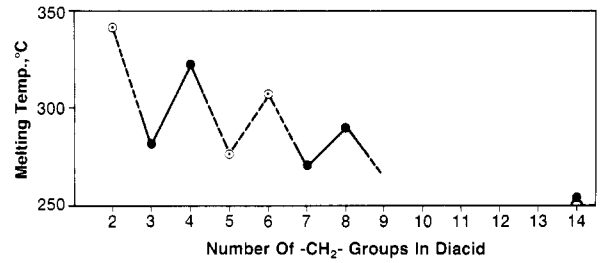

Figure 3. Transition map of the $y = 2$ poly(ester amide) family: (●) experimental; (○) extrapolation. Crystalline polymer below the saw-tooth curve; isotropic melt above it.

of the $y = 2$ family is shown in Figure 3. It clearly shows substantial odd–even effects, where the poly(ester amides) with even-numbered ($x = 2n$) methylene groups between the amide residues exhibit higher melting points than their odd-numbered neighbors. Such an odd–even effect was found to hold true for all other poly(ester amides) in Table I.

The situation is dramatically different in the case of the poly(ester amides) with $y = 3$, 4, 5, and 9, in Table I. All members of these families, with the exception of $y = 4$ and $x = 2n$, showed two or more reproducible first-order transitions upon heating from ambient to the isotropic melt temperature. In the case of $y = 4$, $x = 2n$, only one endothermic transition, melting to the isotropic state, was observed. Most of the multiple transitions were observed by both DSC and microscopy scans, but there were a few which were obvious by one technique and practically invisible by the other. Thus, for example, a low-temperature softening transition, T_s, was noticeable by an abrupt loss of resilience and slow flow under stress but not by other visible change. In the corresponding DSC scans this transition was only occasionally observable and then as a small and rather shallow endotherm. Conversely, in instances where x is large, there appeared several small and reproducible endotherms and exotherms above the uppermost major endotherm in the heating cycle of the DSC scans. These transitions were hardly noticeable by cross-polarized light microscopy.

A DSC scan of the $y = 3$, $x = 4$ poly(ester amide) is shown in Figure 4. This scan is typical of most poly(ester amides) where x is small, say $\leq x \leq 4$. For these polymers the cooling curves show no transitions, and upon reheating the lowest endotherm (214 °C in Figure 4) fails to reappear. Figure 5 shows a DSC scan for the poly(ester amide) $y = 3$, $x = 8$ which is characteristic of polymers where $5 \leq x \leq 8$. Here, both major endotherms reappear in the second and subsequent heating cycles. In the cooling cycle, there

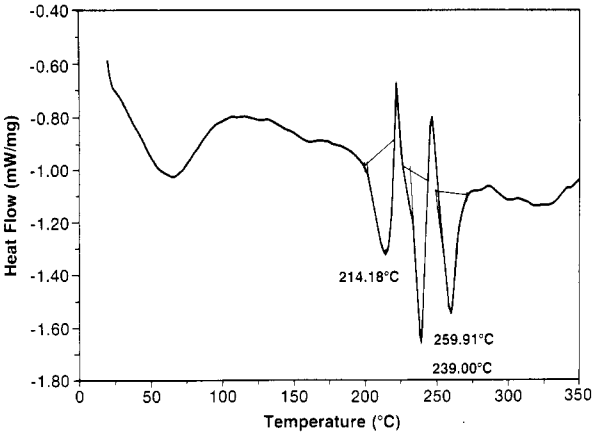

Figure 4. Heating cycle of DSC scan of poly(ester amide) with $y = 3$, $x = 4$.

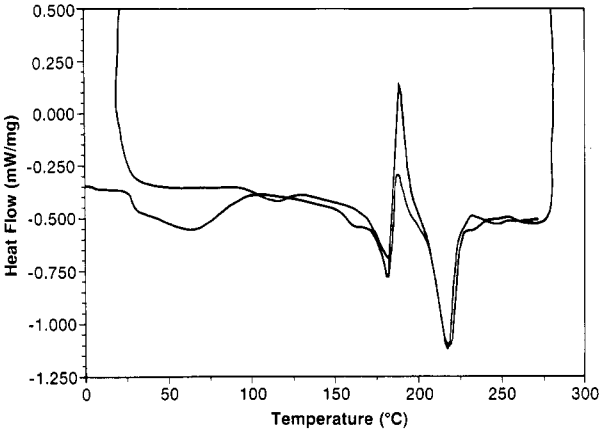

Figure 5. First and second heating cycles in DSC scan of poly(ester amide) with $y = 3$, $x = 8$.

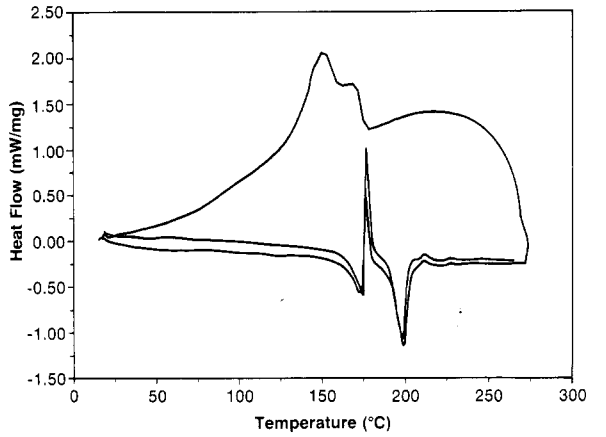

Figure 6. Heating, cooling, and reheating cycles in DSC scan of poly(ester amide) with $y = 3$, $x = 14$.

usually appears only one exotherm which is substantially supercooled relative to the uppermost major endotherm. In Figure 6, a complete sequence of heating, cooling, and reheating is shown for the poly(ester amide) $y = 3$, $x = 14$. This is rather typical of all polymers where $10 \leq x \leq 14$. It is obvious that in the two heating cycles both the major and minor endotherms and exotherms reproduce extremely well. In the cooling cycle, an abrupt ordering takes place at no supercooling relative to the major ordering exotherm in the heating cycles. This is considered[16] to be characteristic of mesomorphic transitions. In Figure 7, a magnified portion of the first heating cycle from Figure 6 is shown. The small transition at about 124 °C is not re-

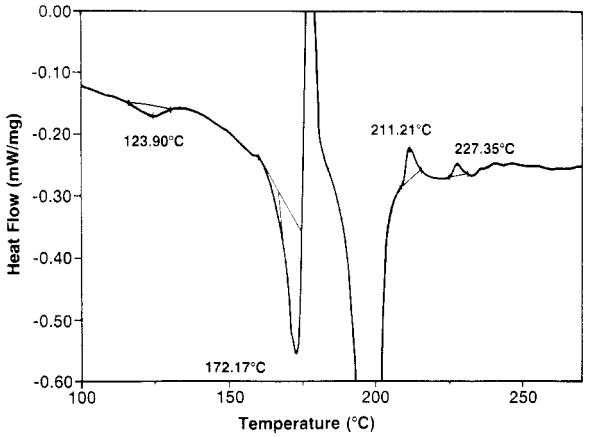

Figure 7. Magnified portion of the first heating cycle in Figure 6.

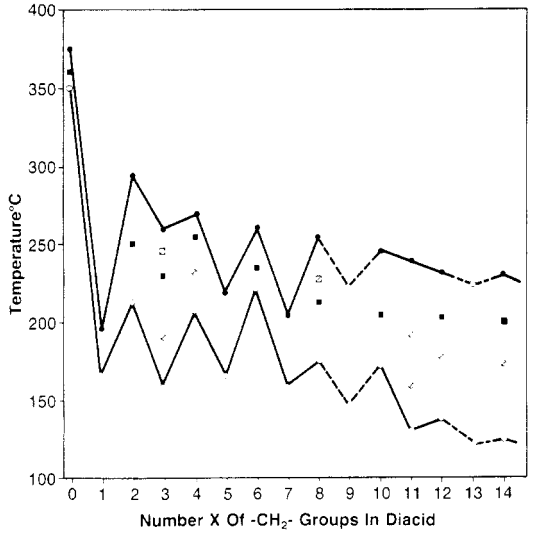

Figure 8. Transition map of the $y = 3$ poly(ester amide) family: (●) isotropization temperature; (○) softening temperature (above T_g); (■) onset of spontaneous flow of intensely birefringent polymer; (□, ⊖) additional transitions.

produced in the second and subsequent heating cycles. It corresponds to the softening temperature observed by the application of pressure during microscopy studies. Above the uppermost major endotherm (ca. 195 °C), at least two small exotherms are visible, which are reproducible in subsequent heating cycles.

In all cases where high-temperature small exotherms were observed by DSC during the heat cycle, intense birefringence of the soft poly(ester amides) became very noticeable at lower temperatures, usually at the uppermost major endotherm or upon approaching the first higher small exotherm. The birefringence persisted through all the small transitions, but at this temperature interval it was substantially duller than before. Finally, it faded away at a temperature above the uppermost small transition. When $y = 3$ and $x + y = 2n + 1$ (odd), a spontaneous flow of the poly(ester amides) was observed in at least part of the temperature interval where intense birefringence was visible. This behavior was found to hold also for $y = 3$, $x = 3$ where $x + y = 2n$ (even). In the family of $y = 4$, intense birefringence coupled with spontaneous flow appeared for the members with $x = 5$, 7, and 11 but not for $x = 3$. The $y = 5$ family follows the behavior of the $y = 3$ family: all polymers with $x + y = 2n + 1$ and $y = 5$, $x = 11$ show intense birefringence with spontaneous flow while the members with $x + y = 2n$ (except for $y = 5$, $x = 11$) develop intense birefringence upon softening but no

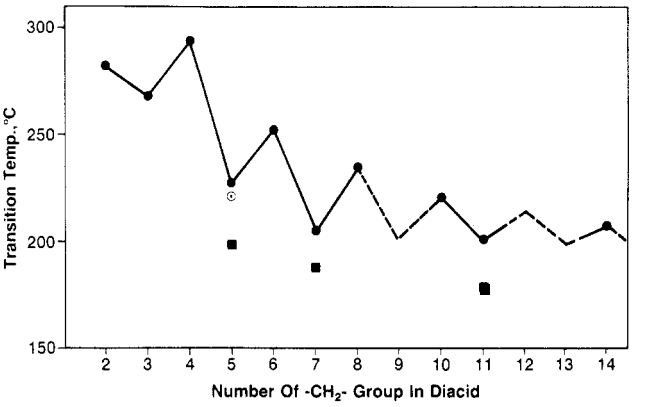

Figure 9. Transition map of the $y = 4$ poly(ester amide) family: (●) isotropization temperature; (■) onset of spontaneous flow of intensely birefringent polymer; (○) second first-order transition.

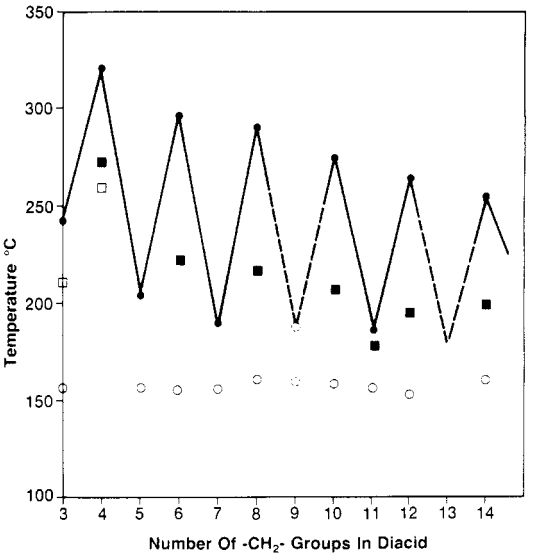

Figure 10. Transition map of the $y = 5$ poly(ester amide) family: (●) isotropization temperature; (○) softening temperature above T_g; (■) onset of spontaneous flow of intensely birefringent polymer; (□) birefringence without spontaneous flow. Dashed circles are extrapolated.

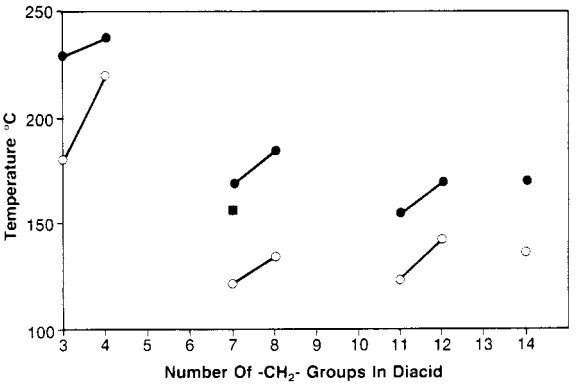

Figure 11. Transition map of the $y = 9$ poly(ester amide) family: (●) isotropization temperature; (○) softening temperature; (■) onset of spontaneous flow of intensely birefringent polymer.

spontaneous flow. Among the members of the $y = 9$ family, intense birefringence coupled with abrupt softening appears throughout, but spontaneous flow was observed only in the case of $y = 9$, $x = 7$, which is a deviation from the $x + y = 2n + 1$ rule. Figures 8, 9, 10, and 11 are transition maps of the $y = 3$, 4, 5, and 9 families, respectively. The existence of multiple endotherms in the DSC

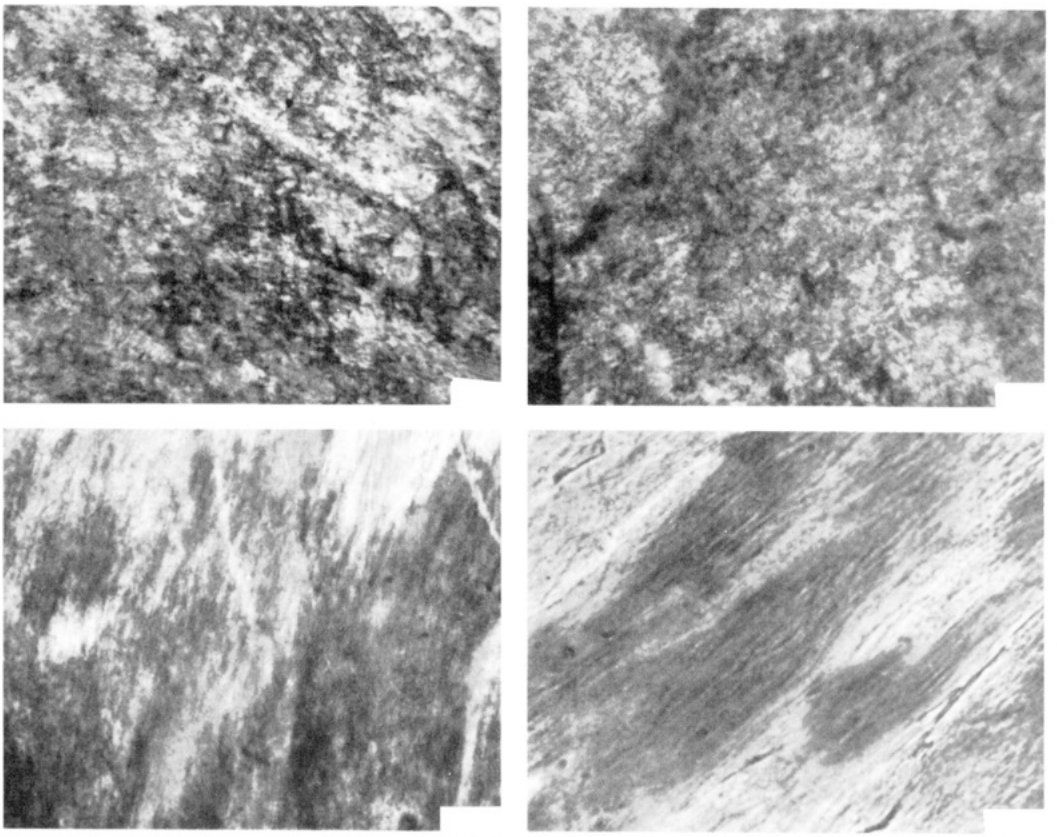

Figure 12. Cross-polarized light micrographs of films of poly(ester amide) $y = 3$, $x = 4$ molded at 275 °C and quick quenched to 0 °C. Top panels are at 54× magnification, left bottom panel is 192× magnification, and bottom right panel is at 378× magnification.

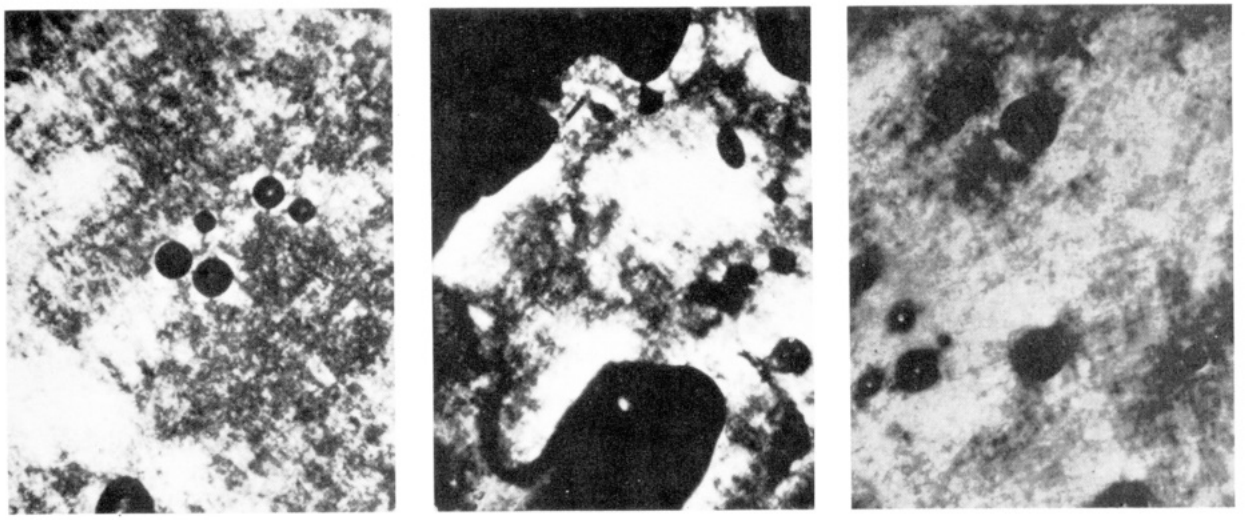

Figure 13. Intensely birefringent, flowing poly(ester amide) $y = 3$, $x = 8$ at 230 °C. Dark areas are air bubbles or have no sample in them.

heating scans concomitantly with a birefringent flowing mass in between or above these transitions is taken to indicate the presence of thermotropic liquid crystallinity. Thus, we conclude that the poly(ester amides) with y = 3, 4, 5, and 9 exhibit mesomorphic behavior. The onset of spontaneous fluidity for $x + y = 2n + 1$ may indicate that more than one liquid-crystalline form exists for these polymers.

Provided the poly(ester amides) passed through the isotropic melt state, the texture of the birefringent mass flowing under stress or spontaneously in the heating cycles is different from the texture during the cooling cycles. The textures are also dependent on the length of the alkylene group in the diacid comonomer, i.e., on x. When poly(ester amides) with small x show upon heating intense birefringence with or without spontaneous flow, the birefringent mass appears featureless with grainy texture. This highly mobile, intensely birefringent grainy mass remains almost unchanged until the birefringence fades over a narrow temperature interval at the isotropization (clearing) point, T_i. The appearance of the grainy texture is clearly apparent in the lower magnification panels of Figure 12, obtained from quick quenched (>500 K/min) films of the poly(ester amide) $y = 3$, $x = 4$ molded at 275 °C, right below T_i. Under high magnifications elongated features indicative of substantial orientation become visible. However, a few minutes stay in the isotropic melt state completely erases both the crystallinity and the grainy texture and films of poly(ester amides) with small x quick quenched from the isotropic melt are amorphous.

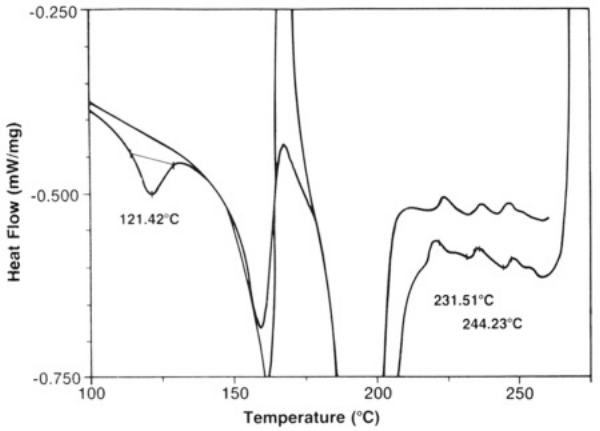

Figure 14. Magnified portion of the two heating cycles in the DSC scan of poly(ester amide) $y = 5$, $x = 14$. Notice the disappearance of the small transition at 121.4 °C and the reproducibility of all other, major and minor, endotherms and exotherms.

Except for the occasional appearance of small needlelike entities in the flowing mass, no fundamental change in the birefringent texture takes place with increases in x to around 8. Figure 13, for the poly(ester amide) $y = 3$, $x = 8$ is typical. It was obtained at 230 °C, above the uppermost major endotherm of the polymer. The white areas in the micrographs are the birefringent and flowing poly(ester amide). The dark round inclusions are air bubbles. Occasional minute needlelike particles are visible in the left panel. Quick-quenched films of the poly(ester amides) $y = 3$, $x = 8$ and $y = 3$, $x = 7$ molded in the mesomorphic interval a little below T_i show essentially the same polychromic grainy texture shown above in the low-magnification panels of Figure 12 for the poly(ester amide) $y = 3$, $x = 4$.

As x further increases, small transitions above the uppermost major endotherm become more and more noticeable. In Figure 6 it was shown that these minor transitions are reproducible upon heating (as long as the heating and cooling rates are 10 K/min or less). This reproducibility is more clearly visible in a magnified portion of two heating cycles in the DSC scan of the poly(ester amide) $y = 5$, $x = 14$, in Figure 14. Here, the three small exotherms and intervening shallow endotherms are clearly visible in both heating cycles. Figure 14 is typical of poly(ester amides) with $10 \leq x \leq 14$. With the pronounced appearance of small transitions above the uppermost major endotherm, a change in the birefringent textures occurs. Upon heating, an intensely birefringent fluid mass appears between the two major endotherms or, occasionally, around the uppermost major endotherm. With further heating, usually around one of the lower small exotherms, the intense birefringence is replaced by a dull birefringence which remains until the sample fully extinguishes the cross-polarized light at T_i. The texture of the intensely birefringent mass is featureless and somewhat grainy, with an occasional appearance of minute rodlike entities. In the dull birefringent interval, very small iridescent specs appear to be floating and tumbling in an extinguishing melt. The textural changes of the poly(ester amide) $y = 3$, $x = 10$ can clearly be followed in Figure 15. At 170 °C the material is solid, right at the softening point. The two panels at 222 and 225 °C show the intense birefringence of the mesomorphic phase after spontaneous flow started. At 240 °C we are in the dull birefringent phase, below T_i.

Annealing the dull birefringent samples isothermally for up to 90 min failed to cause any change in them. The minute birefringent specs did not vanish, nor did they grow

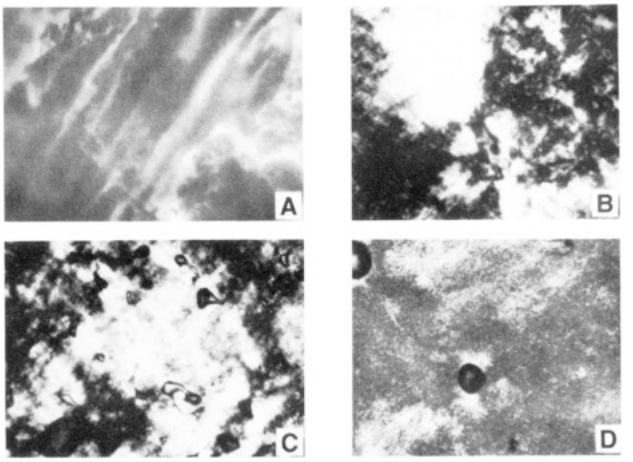

Figure 15. Textural changes of poly(ester amide) $y = 3$, $x = 10$ during a heating cycle: (A) during softening, at 170 °C; (B and C) intensely birefringent flowing polymer at 222 °C and 225 °C, respectively; (D) dull birefringence at 240 °C.

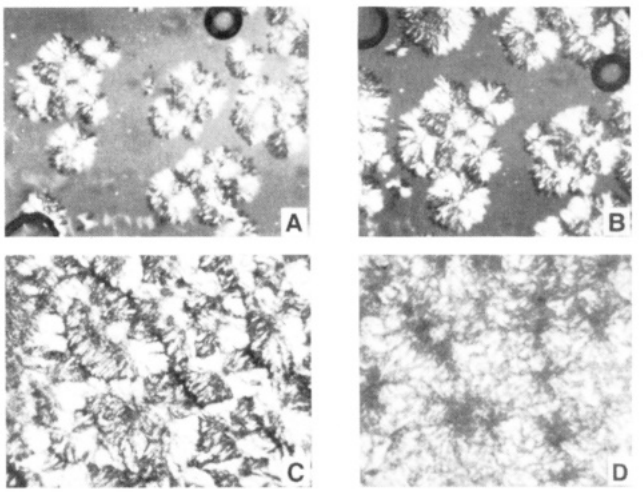

Figure 16. Textural changes of poly(ester amide) $y = 3$, $x = 14$ upon cooling from 250 °C: (A) ordered structures appear at 210 °C; (B) after 5 min at 210 °C; (C) the whole field of vision filled with ordered structures, after ca. 20 min at 210 °C; (D) abrupt textural change with strong exotherm at 180 °C, same area as in (C).

in size or coalesce or change in any manner. However, when poly(ester amides) with large x were heated to their isotropic melt state, kept there from a few minutes up to an hour, and then cooled down at a rate of 10 K/min or slower to the same isothermal anneal temperature as before, dramatic growth of birefringent entities started within minutes or even seconds. This is especially remarkable because in some poly(ester amides) the growth of ordered structures upon cooling started at temperatures of 40–50 °C above the uppermost major endotherm in the corresponding heating cycle. A typical example for such a behavior is the poly(ester amide) $y = 3$, $x = 14$. In its heating cycle there appear two major endotherms at about 172 and 200 °C and one major exotherm at about 177 °C. The lowest endotherm signifies a complete or partial melting of one crystalline form, C_1, while the upper endotherm is associated with the onset of spontaneous flow and intense birefringence. The 177 °C exotherm indicates a crystallization of the C_2 modification taking place. At about 212 °C the intense birefringence changes, with a small exotherm, into dull birefringence which fades into an isotropic melt at 235 °C, above several small transitions. The DSC scans of $y = 3$, $x = 14$ are very similar to those of $y = 5$, $x = 14$ in Figure 14. Upon cooling from the isotropic melt

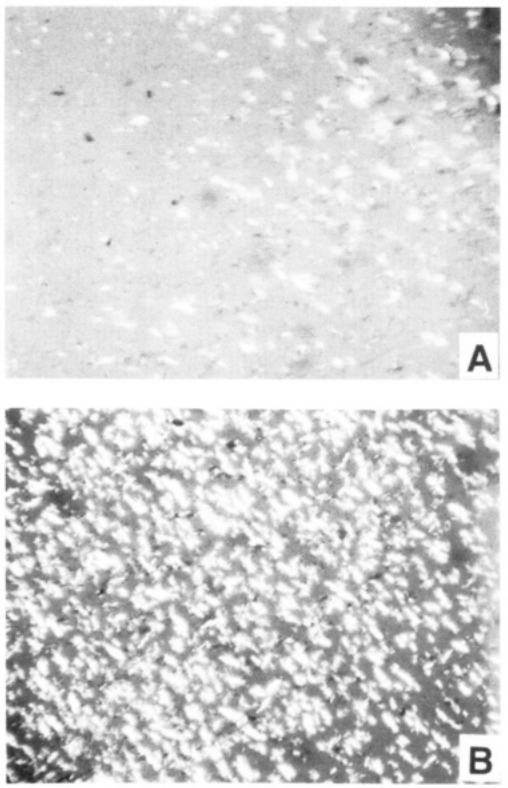

Figure 17. Growth of batonnet-like structures upon cooling of poly(ester amide) $y = 5$, $x = 10$ from isotropic melt at 280 °C. (A) Batonnets start appearing at 255 °C; (B) upon further cooling to 225 °C.

and isothermal anneal at 210 °C, very fine elongated brushlike structures appear which rapidly thereafter change habit and grow into spherulites of substantial size (Figure 16A,B). When allowed enough time at the anneal temperature, the spherulites grow more in size and less so in number and fill the whole field of vision (Figure 16C). Upon cooling to 180 °C, an abrupt change in morphology takes place and the whole volume of the sample fills with fine crystalline material. Even though the spherulites appear to have broken down to a much finer texture, their gross features can still be faintly discerned (Figure 16D).

The development of large ordered structures in cooling poly(ester amides) with large x is even more dramatic when $y = 5$. Upon cooling from the isotropic melt at 280 °C of the poly(ester amide) $y = 5$, $x = 10$, ordered structures which best can be called batonnets start appearing in the flowing melt at 255 °C. With further cooling, their number rapidly increases, but not their size. These ordered structures are highly mobile in the isotropic melt in which they are immersed. Parts A (255 °C) and B (225 °C) of Figure 17 are typical. The ordered structures all appear high in the temperature interval where flowing intense birefringence is present during the heating cycle. With further reduction of temperature, a phase transition occurs at about 200 °C and apparently crystalline structures fill the sample volume.

Figure 18 is a composite of the DSC and microscopy observations for the poly(ester amide) $y = 5$, $x = 11$. Such composites were prepared for many other poly(ester amides) and were used for the purpose of performing variable-temperature and the corresponding quick-quenched ambient temperature WAXD scans. Several composites are shown below. Here, C_1 and C_2 stand for two crystalline modifications, I stands for the isotropic melt, T_g is the glass transition temperature, the vertical solid lines and their length are the DSC transitions and approximations of their

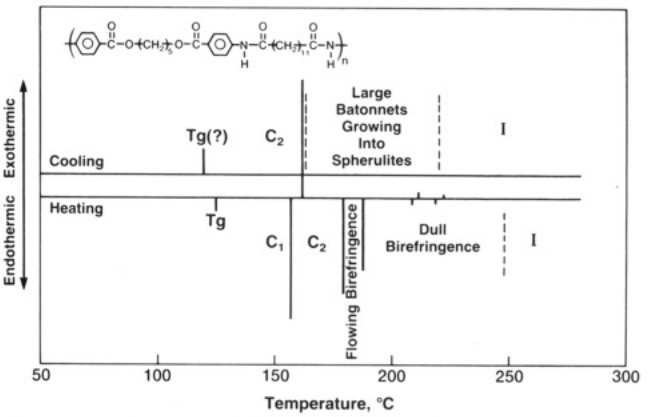

Figure 18. Composite DSC/microscopy diagram of poly(ester amide) $y = 5$, $x = 11$. Heating and cooling at 10 K/min.

intensities, and the dashed lines represent transitions observed by microscopy. Upon cooling the $y = 5$, $x = 11$ polymer from the melt and isothermally annealing at 210 °C for a few minutes, swarms of batonnets appear. These not only flow in the melt but seem to vanish and reform rapidly. The appearance of the batonnets at 210 °C is shown in Figure 19. When the sample is cooled to below 180 °C, the batonnets start growing secondary side arms and change into spherulites. These convert abruptly at ca. 160 °C into a different, fine-textured crystalline structure. A similar behavior occurs with the poly(ester amide) $y = 5$, $x = 14$. We follow the changes occurring in this polymer in Figure 20. Panel A, taken upon heating at 180 °C, shows the intense birefringence as it exists above the softening temperature but below the point where spontaneous flow takes place. The dark areas in the micrograph are areas where no sample was present. Panel B was taken during the heating cycle at 210 °C and in its lower part the flowing birefringent polymer is clearly visible. Panel C, obtained upon heating at ca. 235 °C, shows the dull birefringent fluid with the fine-grained birefringent specs filling it. This texture persisted through several minor transitions until it faded away at about 255 °C. After about 15-min residence in the isotropic melt at 270 °C, the sample was cooled at 10 K/min with occasional isothermal annealing for the purpose of obtaining micrographs. Anywhere in the interval between 245 and 200 °C ordered structures appear within a few minutes. They first appear as rather large batonnets, many with fine fibrillar tips. These usually ripen into crosslike structures. In panel D, obtained at 235–230 °C upon cooling, several such batonnets and crosslike structures are prominent. When allowed to anneal isothermally for 20–30 min, the number of ordered structures increases but their size remains about constant (panel E). Note that the temperature at which these ordered structures appear is up to 45 °C above the uppermost major endotherm in the heating cycle. Upon further cooling to below 200 °C, corresponding to the uppermost major endotherm, fine needlelike and fine-grained birefringent entities appear in the extinguishing areas between the large structures. This mixture of ordered structures is visible in panel F. With further cooling, to below 168 °C, the sample undergoes a phase transition to a finer grain crystalline form, in panel G.

A literature survey indicates that many of our microscopy observations and some features of the DSC scans are not different from what was previously reported. Thus, the disappearance upon reheating of the small and shallow endotherm, apparently associated with the softening point, is reminiscent of similar observations.[38-40] As we shall demonstrate later, in our case this is associated with the

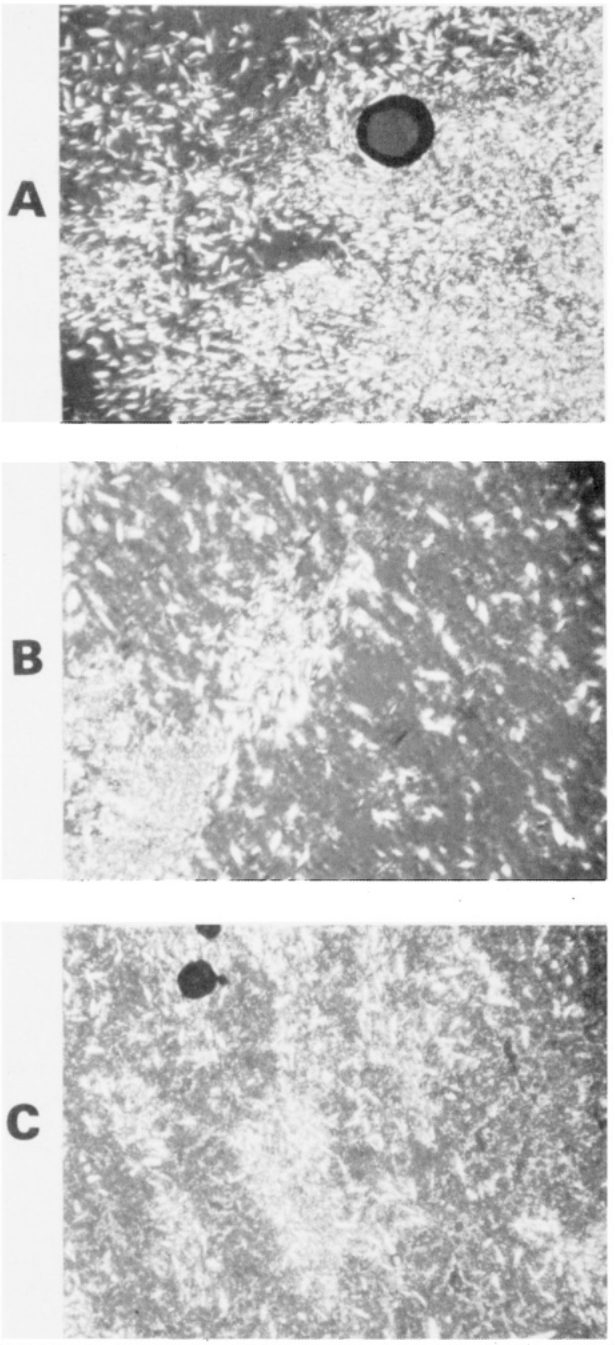

Figure 19. Appearance of batonnets upon annealing at 210 °C of poly(ester amide) $y = 5$, $x = 11$ after cooling from the isotropic melt at 270 °C. At this point the system is remarkably fluid.

replacement of an unstable crystalline modification, C_1, by a stabler modification, C_2, in Figure 18. The textures of the intense and dull birefringent flowing masses we noted so often during the heating cycles are similar to many micrographs and statements in the literature.[41-43] They are commonly attributed to high melt viscosity, as is indeed the case with our poly(ester amides). As can be seen from the DSC scans in Figure 6 and the composite diagram in Figure 18, there appear to be no DSC-discernible transitions in the cooling cycle at the points where ordered structures developed in the melt. This phenomenon is uncommon but not extraordinary, since it was previously observed in several PLC's.[44-48] Finally, the development upon cooling only and not upon heating of distinct mesomorphic texture in the mobile isotropic phase, in our case elongated batonnets or batonnet-like or rodlike or fine brushlike structures, is well documented in the literature[49,50] and is not exceptional. In fact, the smectic batonnets for a polyester shown in Figure 12 of ref 50 are almost identical in appearance with some of ours.

To check on the length of x still producing thermotropic liquid crystallinity, the poly(ester amides) $y = 3$, $x = 20$ and $y = 5$, $x = 20$ were prepared by the Yamazaki procedure. Their intrinsic viscosities were 0.70 and 0.37 dL/g, respectively, indicating modest to high molecular weights. The $y = 3$, $x = 20$ polymer had only one endotherm in its DSC heating scan and showed no mesomorphicity by microscopy. The poly(ester amide) $y = 5$, $x = 20$ exhibited in the first heating cycle two major endotherms followed by several small ones, but only one major endotherm in subsequent cycles. Spontaneous flow of birefringent mass appeared in the first heating cycle at the peak of the uppermost major endotherm (169 °C). The intense birefringence turned dull at 188 °C and faded away at 228 °C. Upon cooling, ordered structures appeared at temperatures higher than either of the major endotherms. Reheating from room temperature failed, however, to reproduce the mesomorphic behavior observed in the first heating cycle. We conclude that the poly(ester amide) $y = 5$, $x = 20$ is marginal in its mesomorphic behavior. The above indicates that 20 is probably the upper limit of x for liquid-crystalline behavior of the poly(ester amides).

Based on the above we conclude that the strictly regular, alternating poly(ester amides) exhibiting several reproducible endotherms and exotherms in their DSC heating scans, combined with the appearance of mobile intense birefringence with or without spontaneous flow and dull birefringence for large x, are indeed liquid crystalline. Among these, with very few exceptions, are the poly(ester amides) with $y = 3$, 5, and 9 and x in the range 1–14. $x = 20$ is a marginal case. The polymers with very small x or with $y = 9$ are less well-behaved than other members of this broad family. In the case where $y = 2$, no mesomorphic behavior was detected. Polymers with $y = 4$, $x = 2n + 1$ generally produced mesomorphicity while $x = 2n$ did not. The best range for mesomorphicity is, hence, $y = 3$ and $y = 5$ with $5 \leqslant x \leqslant 14$.

(c) Infrared. Infrared spectra were obtained at room temperature from the poly(ester amides) with $y = 2$, $x = 7$; $y = 3$, $x = 3$, 4, 7, 8, 11, 12; $y = 4$, $x = 8$; and $y = 5$, $x = 7$, 8, 14. Variable-temperature spectra at selected temperatures in the range 25–270 °C were obtained from $y = 3$, $x = 3$, 4, 7, and 8. Spectra were also obtained from bis(*p*-aminobenzoyl)propane and the model compound prepared from it and nonanoic acid. A detailed analysis of the IR spectra will be published elsewhere, but the salient features of portions of the spectra are given below. In general, there exists a remarkable similarity among the room temperature spectra, except for the bands associated with aliphatic and aromatic C–H bonds changing their intensities essentially according to the amounts present of methylene and aromatic groups. There exists in the spectra a broad dominant band in the range 3350–3300 cm^{-1}. The peak position of this band changes slightly with changes in the poly(ester amide). Increases in temperature entail slight increases in the frequency of this band and some broadening. This broad N–H stretch band is characteristic of the hydrogen-bonded (H-bonded) trans form of the amide group. Occasionally one observes an extremely weak shoulder at about 3400 cm^{-1}, which is characteristic of nonbonded free N–H stretching. The above indicates that all or almost all of the amide groups in the poly(ester amides) are H-bonded. The variations in peak position, intensity, and breadth of the H-bonded N–H stretch band reflect, we believe, changes in H-bond

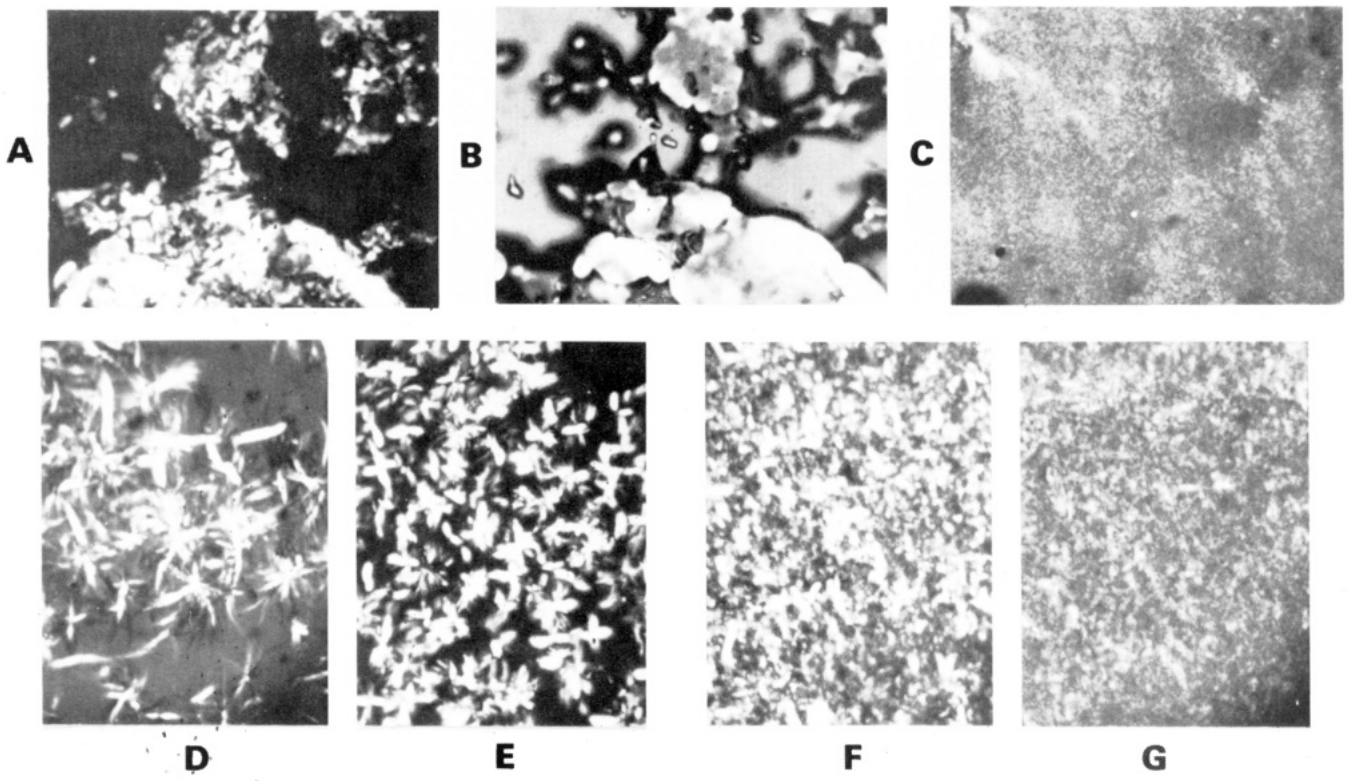

Figure 20. Textural changes during heating and cooling of poly(ester amide) $y = 5$, $x = 14$. Explanation in text.

strength more than an increase in the population of unbonded N–H at the expense of the H-bonded N–H. This is not firmly proven yet but is in keeping with the recent work of Coleman and associates[51,52] on hydrogen bonding in polymers.

The ester carbonyl–amide I region (1750–1630 cm^{-1}) is complex, with four or more observable bands. An intense band at 1720–1710 cm^{-1} is typical for aromatic ester carbonyl groups. Upon heating, an additional band appears at ca. 1710–1705 cm^{-1}. An additional band at ca. 1695 cm^{-1} is assigned as an ester carbonyl band since it appears as a major band in the spectrum of bis(*p*-aminobenzoyl)-propane and since it does not undergo frequency and intensity changes with temperature in between T_s and T_i of the poly(ester amides). These assignments were all verified by comparison of the spectra of the poly(ester amides) with that of the poly(ether amide) with $y = 3$, $x = 8$. In the latter case one observes the prominent amide I band at 1655 cm^{-1}, amide II band at ca. 1530 cm^{-1}, and H-bonded N–H stretch at 3300 cm^{-1}, but no bands at all in the ester carbonyl interval from, say, 1670 to 1750 cm^{-1}. In the poly(ester amides) the amide I band appears at ca. 1660 cm^{-1}. An additional band appears near 1680 cm^{-1} upon heating. Both these bands undergo pronounced frequency and intensity shifts and are assigned to the H-bonded amide carbonyl. These amide I band positions are higher than those observed[52] for aliphatic polyamides by about 10 cm^{-1}, but this is expected in light of the proximity of an aromatic ring to the amide groups in the poly(ester amides). The 1680-cm^{-1} band may be associated with unbound amide carbonyls or with H-bonded ones where the bonds are greatly weakened. Nevertheless, on the basis of the N–H stretching, H-bonding dominates the structure at elevated temperatures, even high in the molten isotropic state.

Importantly, the IR spectra indicate that for each polymer abrupt changes in the intensity and frequency of the amide carbonyl and the ester carbonyl bands appear to occur at the softening point, isotropization temperature,

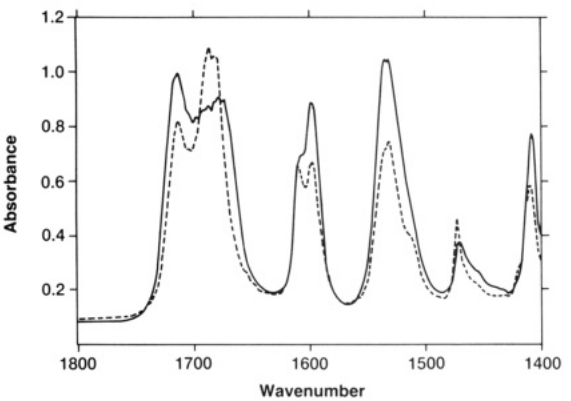

Figure 21. Portions of IR scans of poly(ester amide) $y = 5$, $x = 14$ quick quenched from the mesomorphic state (—) and from the crystalline state (- - -). Notice the broadening and reduction in intensity of the amide I bands of the mesomorphic polymer, at 1650–1700 cm^{-1}, relative to its crystalline phase.

and the intermediate transitions such as the onset of spontaneous flow. Figure 21 is typical of such an abrupt change occurring between the mesomorphic and crystalline phases of the poly(ester amide) $y = 5$, $x = 14$. These abrupt IR alterations are indicative of distinct structural changes but have not been fully interpreted at present.

(d) Wide-Angle X-ray Diffraction Patterns. After synthesis, workup, and drying at around 100 °C, samples were pulverized from most of the poly(ester amides) in Tables I and III and WAXD powder patterns obtained from the as-prepared polymers. Scans were also obtained from several model compounds.

The powder patterns in Figure 22 are typical of poly(ester amides) with $y = 2$. The top panel is for $x = 3$ and typifies all $x \leq 5$ while the bottom panel is for $x = 8$ and is characteristic of all $x \geq 6$. The top and bottom panels in Figure 23 are for the poly(ester amides) $y = 4$, $x = 2$ and $y = 4$, $x = 10$, respectively. They are typical of all $y = 4$, $x \leq 4$ and $y = 4$, $x \geq 5$. Notice the overall similarity

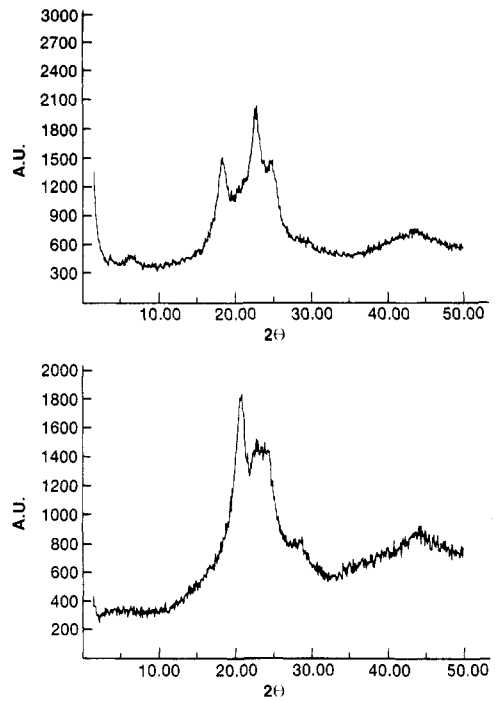

Figure 22. Wide-angle X-ray powder patterns of poly(ester amides) with $y = 2$: (top) $x = 3$; (bottom) $x = 8$.

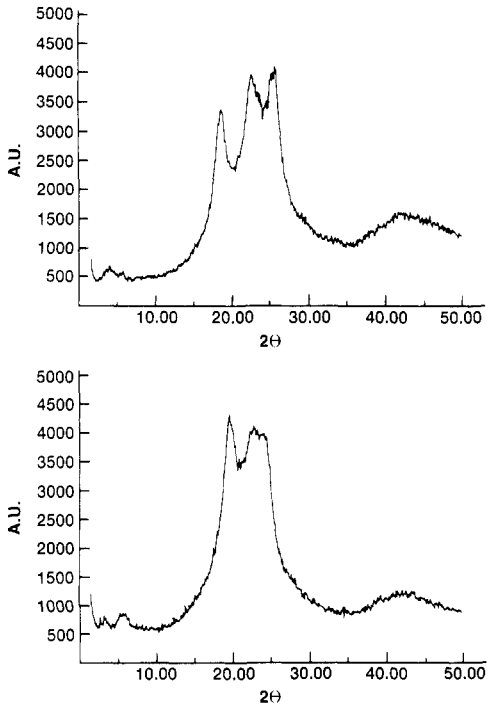

Figure 23. Wide-angle X-ray powder patterns of poly(ester amides) with $y = 4$: (top) $x = 2$; (bottom) $x = 10$.

existing between the two top panels, for small x, and the two bottom panels, for large x. Surprisingly, the WAXD powder patterns for the as-prepared poly(ester amides) with $y = 2$ and $y = 4$ are remarkably similar to those obtained from the as-prepared poly(ester amides) with $y = 9$. Here too, three intense reflections dominate the patterns for small x and change at about $x = 6$ to two intense reflections for large x.

The four panels in Figure 24 are characteristic of as-prepared poly(ester amides) with $y = 3$ and $y = 5$. Panels A and B are for $x = 1$ and $x = 4$, respectively. At $x = 5$, an abrupt change in the WAXD powder patterns is evident and a doublet similar to panels C and D, for $x = 8$ and $x = 12$, dominates. All the as-prepared poly(ester amides) with $y = 3$ and $y = 5$ having $x \geq 5$ exhibited the same high-intensity pattern as panels C and D in Figure 24. Lower intensity reflections at lower angles were routinely present in the powder patterns of the poly(ester amides). In most instances they could be indexed as increasing orders of a large repeat distance, characteristic of each polymer.

Because of the predominance of multiple phase transitions among the poly(ester amides) with $y = 3$ and $y = 5$, because these polymers exhibit most of the observed thermotropic mesomorphicity, and because of the apparent similarity in the WAXD patterns of both as-prepared families, the subsequent X-ray studies were limited to members of these two families only. These studies included flat plate patterns from oriented specimens, variable-temperature studies, and WAXD patterns from quick-quenched samples. The texture of the quick-quenched samples and their high-temperature analogues, observed under a microscope, were essentially identical.[16,53] The same identity became clearly evident in the X-ray studies too. The studies summarized below corroborate the presence of the thermotropic mesomorphicity demonstrated above by DSC and microscopy. This is especially clear in the instances where $y = 3$ or $y = 5$ and x is large ($5 \leq x \leq 14$).

At first glance, the major features of the powder patterns obtained from the as-prepared members of the $y = 3$ and $y = 5$ families with $x \geq 5$ are remarkably similar to the features of powder diagrams obtained from as-prepared aliphatic polyamides in their α-crystalline form. That is, they all have an intense doublet between 20° and 25° 2θ with the inner reflection corresponding to about 4.5 Å and the outer reflection corresponding to about 4.0 Å distances. In studies of polyamides, the larger distance is taken to represent the average distance between H-bonded polyamide chains which form flat or pleated sheets. The smaller distance is the distance between such sheets, controlled primarily by van der Waals interactions.[54] The observation of a reflection in the WAXD patterns that we tentatively identify with H-bonded chains in the as-prepared poly(ester amides) is in agreement with the IR results presented above, indicating a dominance of hydrogen bonding among the amide groups. The apparent presence of H-bonded sheets among the as-prepared large-x members of the $y = 3$ and $y = 5$ families seems to exist among all large x in the $y = 2$, 4, and 9 families. As we move to small x members, the powder diagrams change to a broad three-reflection pattern or to an unsymmetric broad peak apparently consisting of three unresolved peaks. The nature of this broad triplet is not understood at the moment.

The WAXD patterns of poly(ester amides) with $y = 3$ or 5 and $x \geq 8$ crystallized slowly from the melt are different from those obtained from the as-prepared polymers. These new patterns have numerous reflections and, most importantly, the major doublets in the corresponding as-prepared polymers are now replaced by major triplets covering about the same angular range. The top and bottom panels in Figure 25 for the polymer $y = 3$, $x = 8$ are typical examples of the above. The important conclusion to be drawn is that when first prepared, most if not all the poly(ester amides) with $y = 3$ or 5 and large x are obtained in a metastable crystalline form. Exposure to high temperatures ($T \gg 100$ °C) converts them to the stable modification. For clarity and conciseness, we shall denote the metastable crystalline form by C_1 and the stabler crystalline modification by C_2. An example is

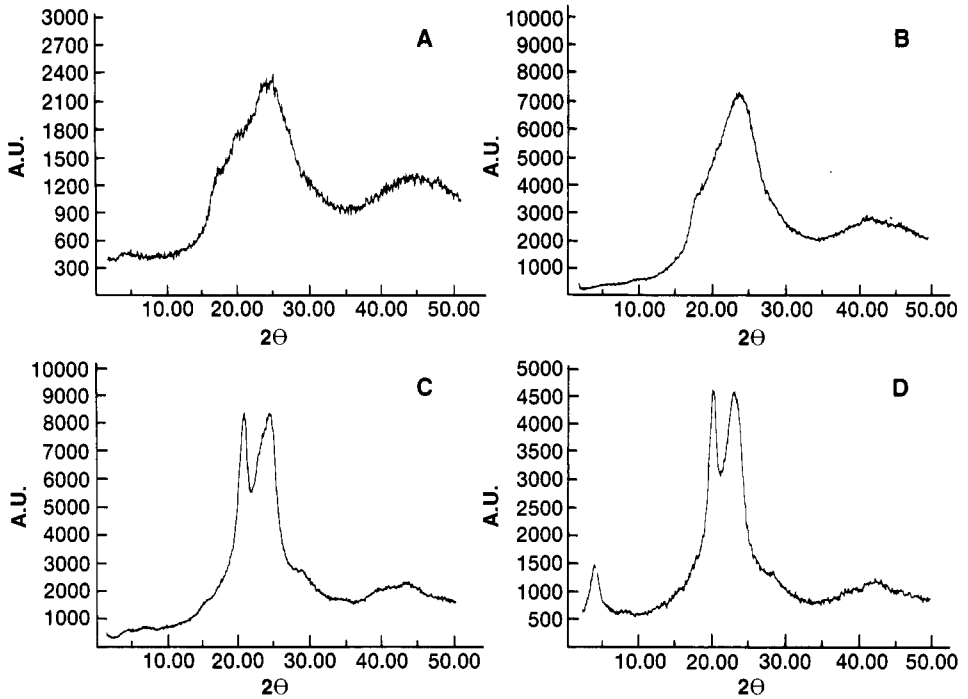

Figure 24. Wide-angle X-ray powder patterns of poly(ester amides) with $y = 3$: (A) $x = 1$; (B) $x = 4$; (C) $x = 8$; (D) $x = 12$. Panels C and D are typical also of poly(ester amides) with $y = 5$ and $x \geq 5$.

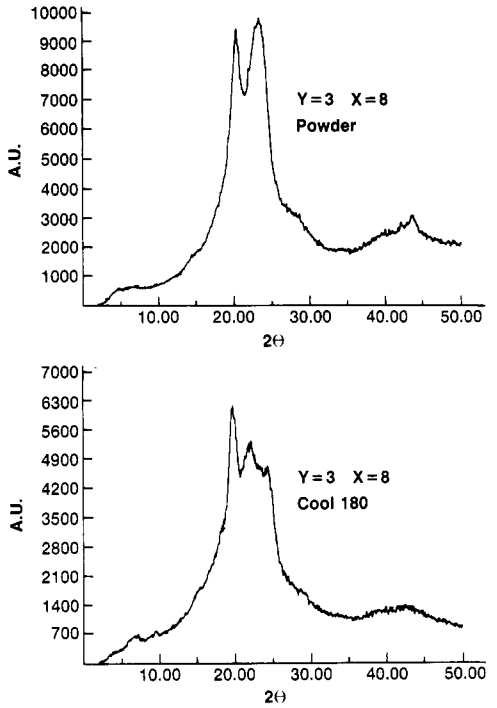

Figure 25. Wide-angle X-ray patterns of poly(ester amide) $y = 3$, $x = 8$: (top) as-prepared, crystalline modification C_1; (bottom) after heating to 270 °C and annealing at 180 °C, crystalline modification C_2.

shown in the composite DSC/microscopy diagram in Figure 18.

In this context, it is interesting to note that when low molecular weight ($0.2 \leq [\eta] \leq 0.3$ dL/g) homologues of the poly(ester amide) $y = 3$, $x = 8$ were prepared and dried at 120 ± 10 °C, their WAXD powder diagrams showed the three intense reflections indicative of the stable C_2 modification. When dried under identical conditions, the higher molecular weight analogues in Table I showed only the metastable C_1 form. The easier transition of the lower molecular weight polymer from the C_1 to the C_2 form is probably due to its lower glass transition temperature, T_g.

Figure 26A is a composite DSC/microscopy diagram of the poly(ester amide) with $y = 3$, $x = 14$. In Figure 26B there appear eight WAXD patterns obtained from samples of the same polymer quick quenched from selected temperatures along the paths of the heating and cooling cycles. Information-wise, these patterns are essentially identical with those obtained at the corresponding temperatures by variable-temperature X-ray measurements and are of higher quality than the latter. Notice the change of the major doublet upon going from C_1 at 160 °C to C_2 at 190 °C. Also note the smooth Gaussian shape of the amorphous halo of the isotropic melt at 250 °C and compare it with the complex and asymmetric shape of the peaks in the liquid-crystalline state both during heating at 205 °C and upon cooling at 200 °C. Finally, note the development of multiple weak reflections at low angles upon heating to C_2 and upon cooling to the practically identical patterns at 160 and 130 °C. The d-spacings associated with the reflections in these last two panels, both intense and weak, are essentially identical with that obtained upon heating to 190 °C. This indicates, as we have seen with all other poly(ester amides) that underwent heat and cool cycling, that upon crystallizing from the cooling melt the stabler crystalline modification, C_2, is obtained. Upon reheating and recooling, the sequence always starts and ends with C_2, and C_1 is not recovered. This X-ray observation is in agreement with the DSC results such as shown in the typical Figure 14. In this case, a transition from C_1 to C_2 is indicated by a small endotherm in the first heating cycle at 121 °C, which is not reproduced in the second heat cycle.

Even more dramatic results were obtained from the poly(ester amide) $y = 5$, $x = 14$. Figure 27A is the composite DSC/microscopy diagram. In Figure 27B, seven panels of WAXD patterns obtained from quick-quenched samples are assembled. These patterns are qualitatively identical with those obtained at the corresponding elevated temperatures. Here, again, the powder diagram is for C_1 and the last panel is for C_2 as obtained upon cooling. The pattern of C_2 obtained during the heating cycle is practically the same as the one obtained upon cooling and is

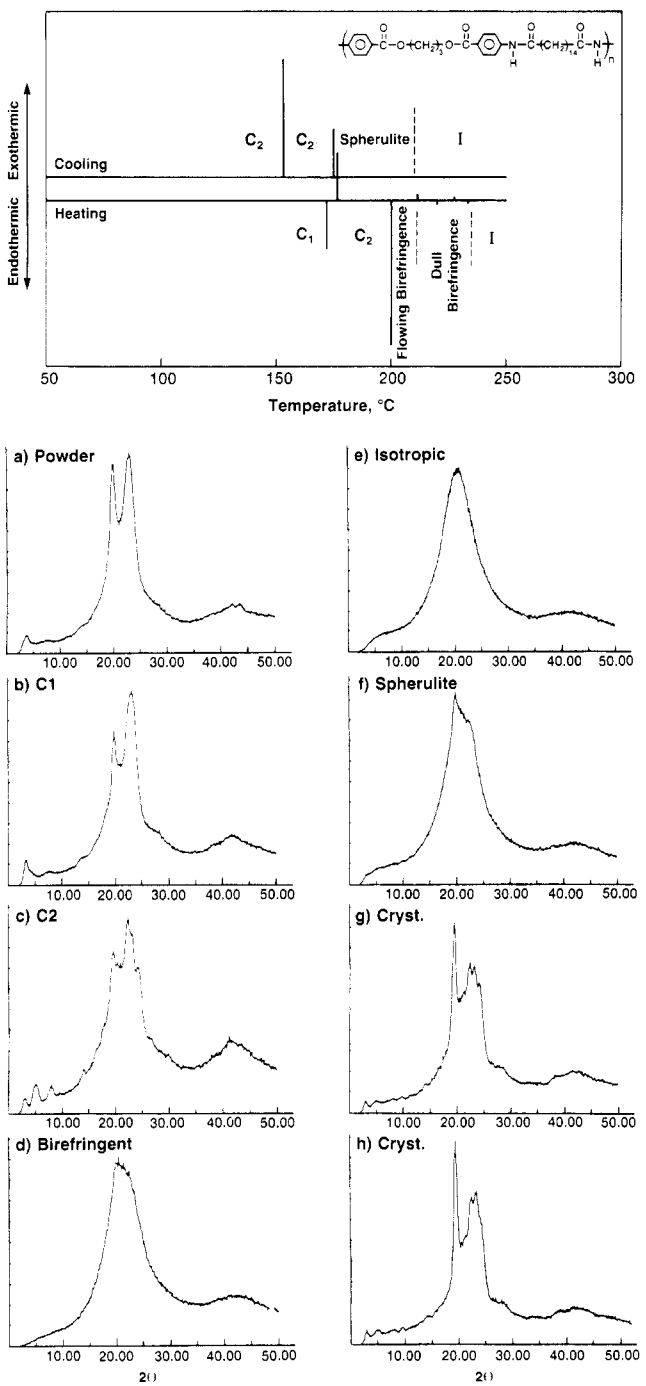

Figure 26. (A, top) Composite DSC/microscopy diagram of poly(ester amide) $y = 3$, $x = 14$. (B, bottom) Corresponding WAXD patterns at the following temperatures: (a) room temperature; (b) heat 160 °C; (c) heat 190 °C; (d) heat 205 °C; (e) heat 250 °C; (f) cool to 200 °C; (g) cool to 160 °C; (h) cool to 130 °C. All heating and cooling at 10 K/min.

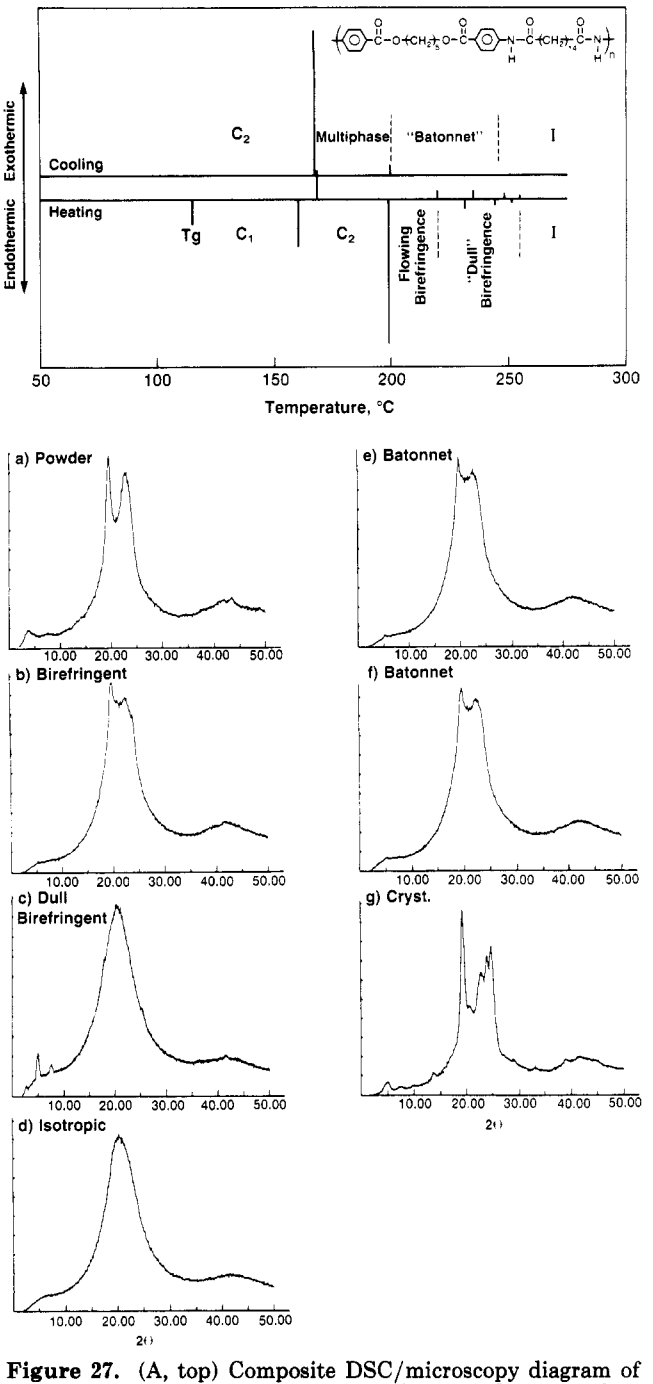

Figure 27. (A, top) Composite DSC/microscopy diagram of poly(ester amide) $y = 5$, $x = 14$. (B, bottom) Corresponding WAXD patterns at the following temperatures: (a) room temperature; (b) heat 215 °C; (c) heat 253 °C; (d) heat 275 °C; (e) cool to 240 °C; (f) cool to 225 °C; (g) cool to 160 °C.

not presented here. In the isotropic state at 275 °C a symmetric Gaussian halo is obtained. In the flowing birefringent (215 °C) and dull birefringent (253 °C) phases below isotropization and in the temperature interval where batonnets make their appearance upon cooling (240 and 225 °C), the major peak is not Gaussian, on occasion its tip is split to more than one reflection, and in the low-angle range one or more weak reflections appear. This last feature is especially spectacular in the dull birefringent, highly fluid state at 253 °C.

The nonsymmetric major diffraction peaks obtained from the birefringent flowing mass upon heating and from the range where ordered structures evolve in the melt upon cooling, together with the appearance of one or more low-angle reflections which are increasing orders of a characteristic large d-spacing, are typical of liquid crystallinity being present in the poly(ester amides). Because such X-ray features were found in most members of the $y = 3$ and $y = 5$ families with $x \geq 7$, we conclude that liquid crystallinity with low levels of order as defined by X-rays exists in all these polymers. The lower x analogues from the $y = 3$ and $y = 5$ families, which exhibit spontaneous flow combined with birefringence, possess rather complex WAXD patterns at the appropriate temperatures, indicative of more ordered structures, the nature of which is unknown at present.

Flat plate X-ray patterns, as well as several meridional and equatorial scans on a Philips diffractometer, were

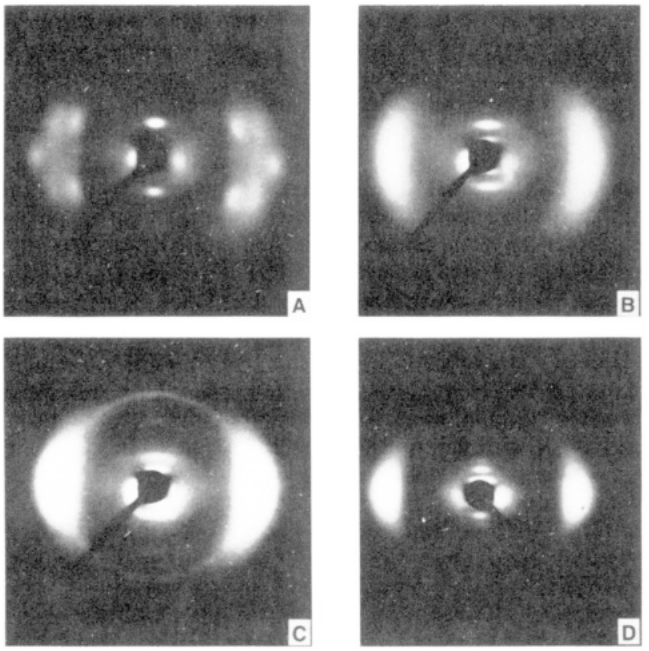

Figure 28. Flat plate X-ray patterns of oriented poly(ester amides): (A) $y = 3$, $x = 4$; (B) $y = 3$, $x = 7$; (C) $y = 3$, $x = 8$; (D) $y = 3$, $x = 14$. Vertical draw direction. In the original flat plates up to eight meridional streaks are visible. The inner unsymmetric equatorial reflection is an artifact due to beamstop scattering and is not inherent to the polymeric samples.

obtained from a few oriented samples. Naturally, the results of both techniques agree well with each other. In Figure 28 are shown four flat plate photographic X-ray patterns obtained from four poly(ester amides). In all cases the draw direction is vertical. Pattern A is for the poly(ester amide) with $y = 3$, $x = 4$. In addition to rather weak and diffuse equatorial reflections and sharper meridional streaks of several orders, there appear several off-equatorial and off-meridional reflections. Patterns B, C, and D are for the poly(ester amides) with $y = 3$ and $x = 7$, 8, and 14. These three patterns are all similar and are each characterized by a diffuse yet intense equatorial reflection, and up to eight orders of sharp meridional reflections. These reflections appear at rather low angle relative to the equatorial reflection. The shape of the meridional reflections is of rather straight streaks. The length of the streaks increases slightly as we proceed from the interior lower orders to the exterior higher orders. Patterns B, C, and D are completely devoid of off-meridional and off-equatorial reflections.

The diffuse equatorial reflections in the three panels correspond to distances of about 4.2 Å. Such distances fall well within the range of interchain, H-bonded amide interactions. The diffuse nature of these reflections indicates a rather poor lateral packing of the chains, resulting in "liquidlike" structure perpendicular to the draw direction. The fact that the equatorial reflection in each of the three panels is a broad singlet indicates that H-bond type interactions are rather random in the planes perpendicular to the average chain direction and are not limited to H-bonded sheets or to well-defined specific directions and distances.

The meridional streaks visible in patterns B, C, and D of Figure 28 are many orders of reflections corresponding to a characteristic large repeat distance along the oriented chains. The mere presence of so many meridional streaks indicates a high level of ordering along the average chain direction, in the draw direction. The combined presence of many sharp meridional streaks and diffuse equatorial reflections stands in dramatic contradistinction to flat plate patterns obtained from oriented aliphatic polyamides where the equatorial reflections are markedly sharper.[55] The repeat distance, L, associated with the streaks in Figure 28B–D, is smaller than the corresponding length, l, of the chemical repeat unit of each poly(ester amide), when it is measured in an all-trans configuration. The fact that $L < l$ and that the meridional streaks are rather sharp and narrow indicates that the chains must be tilted relative to their spatial projection which is responsible for the observed L spacings. The tilt angle changes as we go from $y = 3$, $x = 7$ to $x = 8$ and to $x = 14$ but is in the vicinity of 30°.

An important criterion in deciding whether a given phase has a three-dimensional lattice is the existence of off-meridional and off-equatorial reflections for which all three indices are nonzero.[56] The flat plate pattern in Figure 28A shows the existence of such reflections, indicating the presence of three-dimensional order in the poly(ester amide) $y = 3$, $x = 4$. The very same reflections were clearly observed at 250 °C where the polymer is intensely birefringent and flowing spontaneously, both by the variable-temperature and by the quick-quenched sample procedures. This suggests a three-dimensional order associated with a flowing sample. Such a three-dimensional lattice was shown to exist in several liquid-crystalline phases, namely, smectic G, smectic E and smectic B.[56] At present the exact classification of the liquid-crystalline phase observed in the $y = 3$, $x = 4$ poly(ester amide) cannot be determined. The ambient temperature WAXD patterns of $y = 3$, $x = 4$ are very similar to the patterns of all $y = 3$ and $y = 5$ with $x \leq 4$. Their DSC and microscopy results are also all similar. Therefore, we believe that the polymer $y = 3$, $x = 4$ is typical of all these short-x poly(ester amides).

The absence of off-meridional and off-equatorial reflections from the flat plate patterns of the poly(ester amides) with $y = 3$ and $x = 7$, 8, and 14 indicates that in these polymers there exists no undisturbed two-dimensional lattice perpendicular to the draw direction. The meridional streaks can be treated in terms of several models: (a) tilted smectic C liquid crystals or their twisted analogues,[40,57–59] (b) orthogonal smectic A liquid crystals with rippled layers,[60] (c) paracrystalline layer lattice model,[61,62] and probably (d) the condis (conformationally disordered) crystals.[63] The paracrystalline layer lattice does not produce diffuse equatorial reflections in its diffraction pattern. The rippled smectic A model produces only one meridional reflection which may split into two off-meridional points when the ripple undulation length becomes shorter. This reflection defines a repeat distance L equivalent to the chemical repeat distance l. Both models, hence, are not congruent with our observed patterns. Conversely, diffraction patterns obtained from certain smectic C or twisted smectic C models are in excellent agreement with the patterns obtained from the poly(ester amides) with $y = 3$ and $x = 7$, 8, and 14. Importantly, the appearance of batonnets or elongated structures upon cooling from the isotropic melt, as was repeatedly observed by us, is considered characteristic of the smectic A or the smectic C phases.[16,39,64] The fact that $L < l$ rules out smectic A. Thus, the model we envision is a smectic C or twisted smectic C configuration which is azimuthally disordered with the layers orientationally ordered[40,58] coupled with some axial-shift disorder within the layers.[65] Here, the azimuthal disorder of the segments tilted in the layers produces only meridional reflections with the corresponding L spacings, and the axial-shift

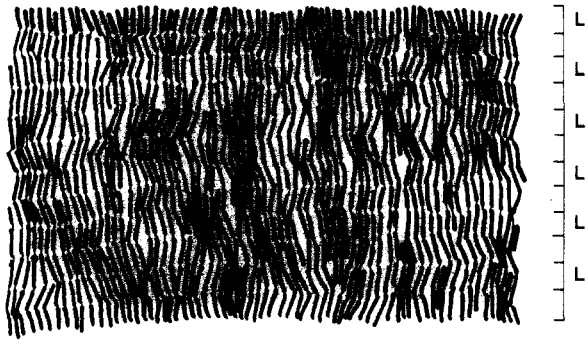

Figure 29. Two-dimensional projection of poly(ester amides) in their smectic C state. Thick lines are the mesogenic units with length l and projection L, H-bonded in planes nearly perpendicular to the average chain direction. Thin lines are the flexible methylene sequences where change in the chain direction takes place.

disorder within the layers makes these reflections adopt the shape of straight streaks that gradually increase in length.[65] This is in agreement with our results. Furthermore, the model dictates a single intense equatorial reflection, corresponding to the average distance between the "parallel" segments. This, too, is in excellent agreement with our diffraction patterns. We speculate that the locus along the chain where it changes direction causing the tilts relative to the layer planes is within the y methylene sequence between the ester groups. This is by analogy with the angular nature adopted by the methylene sequence in crystalline poly(trimethylene terephthalate),[66] which is identical with the $y = 3$ sequence.

Using Chistyakov's[57] model of a smectic structure of low molecular weight materials as the point of departure, we propose, in Figure 29, a two-dimensional projection of the suggested structure of our poly(ester amides) exhibiting smectic C structure. This graphic model accounts for the tilt and azimuthal disorder of the segments within the layers, for the axial-shift disorder of the segments in the layer which disrupts the uniformity of the layers, and for the overall orientational order of the layers as a whole. It is our belief that the model described above reflects the situation not only of the three polymers with $y = 3$ and $x = 7$, 8, and 14 but of all poly(ester amides) with large x ($x \geq 5$) exhibiting liquid crystallinity. The exact nature of the structural changes occurring in the phase transitions is not known to us at present.

(e) Mechanical Properties of Some Fibers Spun from Isotropic Melt. The hydrodynamic radii, R_H, of several poly(ester amides) with $y = 3$ are listed in Table I. Considering the corresponding molecular weights, the radii are rather small. Hydrodynamic radii for flexible chain polymers are known[67] to be between $^2/_3$ and $^7/_8$ the size of their radii of gyration, R_G. However, even the calculated R_G's are relatively small. The smallness of R_H or R_G indicates that in dilute solution the poly(ester amides) behave as simple flexible random coils. This holds true even for the poly(ester amides) with $x = 1$, 2, etc., where rotation around C—C and C—C=O bonds may be somewhat restricted. During extrusion and fiber spinning from the isotropic melt, we have found that our poly(ester amides) possess melt viscosities qualitatively comparable to those of aliphatic polyamides of similar molecular weights. This suggests that in the isotropic molten state the size of the molecular coils of the poly(ester amides) is not greatly different from their size in solution or from the size of comparable polyamides. This observation is in agreement with Blumstein et al.[68] who demonstrated that MCPLC with flexible spacers adopt the same random coil conformation in dilute solution as in the isotropic melt. The spun fibers, from $y = 3$, $x = 7$ and $y = 3$, $x = 8$ were amorphous yet oriented. They developed about 40% crystallinity upon drawing to 5:1. The mechanical properties of the as-spun and drawn fibers appear in Table VI. Interestingly, while the initial modulus of the poly(ester amides) is significantly higher than that of nylon 6, their breaking stress was disappointingly low. The high breaking strains of the spun fibers indicates that their low breaking stress is not due to mere imperfections, impurities, or voids in the fibers.

Table VI
Mechanical Properties of Two Poly(ester amides)[a]

polymer	draw ratio	init modulus, g/denier	breaking stress, g/denier	breaking strain, %
$y = 3$, $x = 7$	undrawn	21.4	0.90	275
	5:1	57.2	3.21	7.7
$y = 3$, $x = 8$	undrawn	19.3	0.75	284
	5:1	56.6	3.80	12
nylon 6	undrawn	9		
	5:1	42	8.9	15

[a] All tests were conducted at 24 °C on fibers equilibrated at 50% relative humidity. Nylon 6 is a high-purity production material, BHS grade, spun as a 14-fiber yarn with total denier of ca. 170 after drawing. The poly(ester amides) were spun as single filaments of drawn denier 26 (for $x = 8$) and 23 (for $x = 7$).

Conclusions

(1) Highly regular, strictly alternating poly(ester amides) are obtained from solution polymerization at moderate or low temperatures. Melt polycondensation leads to scrambled, random polymers.

(2) Thermotropic mesomorphicity, defined as mobile or spontaneously flowing birefringent polymer exhibiting multiple reproducible first-order transitions in the DSC heating cycle, corroborated by X-ray diffraction patterns, is limited to highly regular strictly alternating poly(ester amides) with $3 \leq y \leq 9$ and $1 \leq x < 20$.

(3) Deviations from the regularity and alternation of the poly(ester amides) lead to loss of mesomorphicity. Replacement of amides by esters, or esters by ethers or amides, leads to loss of liquid crystallinity.

(4) There appears to be a consistent structural, and behavioral, difference between poly(ester amides) with $x \leq 4$ and $x \geq 5$.

(5) The most dramatic manifestations of mesomorphicity are given by poly(ester amides) with $y = 3$ or $y = 5$ and $10 \leq x \leq 14$. Upon cooling from the isotropic melt, these develop elongated batonnet-like structures at temperatures far above the uppermost major DSC endotherm.

(6) Infrared scans show that essentially all the amide groups are hydrogen bonded to each other. X-ray patterns indicate these H-bonds are present between chains. The H-bonds are maintained at elevated temperatures.

(7) X-ray patterns from oriented samples and the appearance of batonnet-like structures at elevated temperatures only during cooling from the isotropic melt both indicate that the thermotropic mesomorphicity or poly(ester amides) with $5 \leq x \leq 14$ is, most likely, in the smectic C or twisted smectic C form. For small x ($x \leq 4$) the liquid crystallinity may be of a different form.

(8) A crude model, encompassing all the above features, is proposed.

Acknowledgment. For their aid with various aspects of the experimental work, I thank my colleagues: J. S. Szobota and R. G. Bray (infrared); W. B. Hammond, M. H. Cozine, and A. Kahn (NMR); N. S. Murthy, S. T.

Correale, and H. Minor (X-rays); E. K. Walsh, K. Zero, and C. R. Lombardo (solution properties); J. T. Dunn, M. P. Conroy, and M. F. Martin (synthesis); R. J. Morgan (fiber spinning); N. F. Buik and R. W. Higgins (mechanical testing); J. J. Belles (initial DSC scans); and E. L. Szollosi (initial micrographs). Fruitful discussions with Prof. S. Krimm and Prof. C. Noël are acknowledged.

Registry No. (1,2-Bis(4-aminobenzoyl)ethane)(pentanedioic acid) (copolymer), 114677-07-5; (1,2-bis(4-aminobenzoyl)-ethane)(pentanedioic acid) (copolymer, SRU), 114677-80-4; (1,2-bis(4-aminobenzoyl)ethane)(hexanedioic acid) (copolymer), 114677-08-6; (1,2-bis(4-aminobenzoyl)ethane)(hexanedioic acid) (copolymer, SRU), 114677-81-5; (1,2-bis(4-aminobenzoyl)-ethane)(nonanedioic acid) (copolymer), 114677-09-7; (1,2-bis(4-aminobenzoyl)ethane)(nonanedioic acid) (copolymer, SRU), 114677-82-6; (1,2-bis(4-aminobenzoyl)ethane)(decanedioic acid) (copolymer), 114677-10-0; (1,2-bis(4-aminobenzoyl)ethane)(decanedioic acid) (copolymer, SRU), 114677-83-7; (1,2-bis(4-aminobenzoyl)ethane)(hexadecanedioic acid) (copolymer), 114677-11-1; (1,2-bis(4-aminobenzoyl)ethane)(hexadecanedioic acid) (copolymer, SRU), 114677-84-8; (1,3-bis(4-aminobenzoyl)-propane)(oxalic acid) (copolymer), 114677-12-2; (1,3-bis(4-aminobenzoyl)propane)(oxalic acid) (copolymer, SRU), 114677-85-9; (1,3-bis(4-aminobenzoyl)propane)(propanedioic acid) (copolymer), 114677-13-3; (1,3-bis(4-aminobenzoyl)propanedioic acid) (copolymer, SRU), 114677-86-0; (1,3-bis(4-aminobenzoyl)-propane)(butanedioic acid) (copolymer), 114677-14-4; (1,3-bis-(4-aminobenzoyl)propane)(butanedioic acid) (copolymer, SRU), 114677-87-1; (1,3-bis(4-aminobenzoyl)propane)(pentanedioic acid) (copolymer), 114677-15-5; (1,3-bis(4-aminobenzoyl)propane)-(pentanedioic acid) (copolymer, SRU), 114677-88-2; (1,3-bis(4-aminobenzoyl)propane)(hexanedioic acid) (copolymer), 114677-16-6; (1,3-bis(4-aminobenzoyl)propane)(hexanedioic acid) (copolymer, SRU), 114677-89-3; (1,3-bis(4-aminobenzoyl)-propane)(heptanedioic acid) (copolymer), 114677-90-6; (1,3-bis-(4-aminobenzoyl)propane)(octanedioic acid) (copolymer), 114677-18-8; (1,3-bis(4-aminobenzoyl)propane)(octanedioic acid) (copolymer, SRU), 114677-91-7; (1,3-bis(4-aminobenzoyl)-propane)(nonanedioic acid) (copolymer), 114677-19-9; (1,3-bis-(4-aminobenzoyl)propane)(nonanedioic acid) (copolymer, SRU), 114677-92-8; (1,3-bis(4-aminobenzoyl)propane)(decanedioic acid) (copolymer), 114677-20-2; (1,3-bis(4-aminobenzoyl)propane)(decanedioic acid) (copolymer, SRU), 114677-93-9; (1,3-bis(4-aminobenzoyl)propane)(dodecanedioic acid) (copolymer), 114677-21-3; (1,3-bis(4-aminobenzoyl)propane)(dodecanedioic acid) (copolymer, SRU), 114677-94-0; (1,3-bis(4-aminobenzoyl)-propane)(tridecanedioic acid) (copolymer), 114677-22-4; (1,3-bis(4-aminobenzoyl)propane)(tridecanedioic acid) (copolymer, SRU), 114677-95-1; (1,3-bis(4-aminobenzoyl)propane)(tetradecanedioic acid) (copolymer), 114677-23-5; (1,3-bis(4-aminobenzoyl)propane)(tetradecanedioic acid) (copolymer, SRU), 114677-96-2; (1,3-bis(4-aminobenzoyl)propane)(docosanedioic acid) (copolymer), 114677-25-7; (1,3-bis(4-aminobenzoyl)propane)(docosanedioic acid) (copolymer, SRU), 114677-98-4; (1,3-bis(4-aminobenzoyl)propane)(tetradecanedioic acid) (copolymer), 114677-24-6; (1,3-bis(4-aminobenzoyl)propane)(tetradecanedioic acid) (copolymer, SRU), 114677-97-3; (1,4-bis(4-aminobenzoyl)-butane)(butanedioic acid) (copolymer), 114677-26-8; (1,4-bis(4-aminobenzoyl)butane)(butanedioic acid) (copolymer, SRU), 114677-99-5; (1,4-bis(4-aminobenzoyl)butane)(pentanedioic acid) (copolymer), 114677-27-9; (1,4-bis(4-aminobenzoyl)butane)(pentanedioic acid) (copolymer, SRU), 114678-00-1; (1,4-bis(4-aminobenzoyl)butane)(hexanedioic acid) (copolymer), 114677-28-0; (1,4-bis(4-aminobenzoyl)butane)(hexanedioic acid) (copolymer, SRU), 114678-01-2; (1,4-bis(4-aminobenzoyl)butane)(heptanedioic acid) (copolymer), 114677-29-1; (1,4-bis(4-aminobenzoyl)butane)(heptanedioic acid) (copolymer, SRU), 114678-02-3; (1,4-bis(4-aminobenzoyl)butane)(octanedioic acid) (copolymer), 114677-30-4; (1,4-bis(4-aminobenzoyl)butane)(octanedioic acid) (copolymer, SRU), 114678-03-4; (1,4-bis(4-aminobenzoyl)butane)(nonanedioic acid) (copolymer), 114677-31-5; (1,4-bis)(4-aminobenzoyl)butane)(nonanedioic acid) (copolymer, SRU), 114678-04-5; (1,4-bis(4-aminobenzoyl)butane)(decanedioic acid) (copolymer), 114677-32-6; (1,4-bis(4-aminobenzoyl)butane) decanedioic acid) (copolymer, SRU), 114678-05-6; (1,4-bis(4-aminobenzoyl)butane)(dodecanedioic acid) (copolymer), 114677-33-7; (1,4-bis(4-aminobenzoyl)butane)(dodecanedioic acid) (copolymer, SRU), 114678-06-7; (1,4-bis(4-aminobenzoyl)butane)(tridecanedioic acid) (copolymer), 114677-34-8; (1,4-bis(4-aminobenzoyl)butane)(tridecanedioic acid) (copolymer, SRU), 114678-07-8; (1,4-bis(4-aminobenzoyl)butane)(hexadecanedioic acid) (copolymer), 114677-35-9; (1,4-bis(4-aminobenzoyl)butane)(hexadecanedioic acid) (copolymer, SRU), 114678-08-9; (1,5-bis(4-aminobenzoyl)pentane)(pentanedioic acid) (copolymer), 114677-36-0; (1,5-bis(4-aminobenzoyl)pentane)(pentanedioic acid) (copolymer, SRU), 114678-09-0; (1,5-bis(4-aminobenzoyl)pentane)(hexanedioic acid) (copolymer), 114677-37-1; (1,5-bis(4-aminobenzoyl)pentane)(hexanedioic acid) (copolymer, SRU), 114678-10-3; (1,5-bis(4-aminobenzoyl)pentane)(heptanedioic acid) (copolymer), 114677-38-2; (1,5-bis(4-aminobenzoyl)pentane)-(heptanedioic acid) (copolymer, SRU), 114678-11-4; (1,5-bis(4-aminobenzoyl)pentane)(octanedioic acid) (copolymer), 114677-39-3; (1,5-bis(4-aminobenzoyl)pentane)(octanedioic acid) (copolymer, SRU), 114678-12-5; (1,5-bis(4-aminobenzoyl)pentane)(nonanedioic acid) (copolymer), 114677-40-6; (1,5-bis(4-aminobenzoyl)pentane)(nonanedioic acid) (copolymer, SRU), 114678-13-6; (1,5-bis(4-aminobenzoyl)pentane)(decanedioic acid) (copolymer), 114677-41-7; (1,5-bis(4-aminobenzoyl)pentane)(decanedioic acid) (copolymer, SRU), 114678-14-7; (1,5-bis(4-aminobenzoyl)pentane)(dodecanedioic acid) (copolymer), 114677-42-8; (1,5-bis(4-aminobenzoyl)pentane)(dodecanedioic acid) (copolymer, SRU), 114678-15-8; (1,5-bis(4-aminobenzoyl)pentane)(tridecanedioic acid) (copolymer), 114677-43-9; (1,5-bis(4-aminobenzoyl)pentane)(tridecanedioic acid) (copolymer, SRU), 114678-16-9; (1,5-bis(4-aminobenzoyl)pentane)(tetradecanedioic acid) (copolymer), 114677-44-0; (1,5-bis(4-aminobenzoyl)pentane)(tetradecanedioic acid) (copolymer, SRU), 114678-17-0; (1,5-bis(4-aminobenzoyl)pentane)(hexanedioic acid) (copolymer), 114677-45-1; (1,5-bis(4-aminobenzoyl)pentane)(hexanedioic acid) (copolymer, SRU), 114678-18-1; (1,5-bis(4-aminobenzoyl)pentane)(docosanedioic acid) (copolymer), 114677-46-2; (1,5-bis(4-aminobenzoyl)pentane)(docosanedioic acid) (copolymer, SRU), 114678-19-2; (1,9-bis(4-aminobenzoyl)nonane)(pentanedioic acid) (copolymer), 114677-48-4; (1,9-bis(4-aminobenzoyl)nonane)(pentanedioic acid) (copolymer, SRU), 114678-20-5; (1,9-bis(4-aminobenzoyl)nonane)(hexanedioic acid) (copolymer), 114677-49-5; (1,9-bis(4-aminobenzoyl)nonane)(hexanedioic acid) (copolymer, SRU), 114678-21-6; (1,9-bis(4-aminobenzoyl)nonane)-(nonanedioic acid) (copolymer), 114677-50-8; (1,9-bis(4-aminobenzoyl)nonane)(nonanedioic acid) (copolymer, SRU), 114678-22-7; (1,9-bis(4-aminobenzoyl)nonane)(decanedioic acid) (copolymer), 114677-51-9; (1,9-bis(4-aminobenzoyl)nonane)(decanedioic acid) (copolymer, SRU), 114678-23-8; (1,9-bis(4-aminobenzoyl)nonane)(tridecanedioic acid) (copolymer), 114677-52-0; (1,9-bis(4-aminobenzoyl)nonane)(tridecanedioic acid) (copolymer, SRU), 114678-24-9; (1,9-bis(4-aminobenzoyl)nonane)(tetradecanedioic acid) (copolymer), 114677-53-1; (1,9-bis(4-aminobenzoyl)nonane)(tetradecanedioic acid) (copolymer, SRU), 114691-78-0; (1,9-bis(4-aminobenzoyl)nonane)(hexanedioic acid) (copolymer), 114677-54-2; (1,9-bis(4-aminobenzoyl)nonane)(hexanedioic acid) (copolymer, SRU), 114678-25-0; (1,3-bis(4-aminobenzoyl)propane)((*E*,*E*)-muconic acid) (copolymer), 114677-55-3; (1,3-bis(4-aminobenzoyl)propane)((*E*,*E*)-muconic acid) (copolymer, SRU), 114678-26-1; (1,3-bis(4-aminobenzoyl)propane)(1,4-cyclohexanedicarboxylic acid) (copolymer), 114677-56-4; (1,3-bis(4-aminobenzoyl)propane)(1,4-cyclohexanedicarboxylic acid) (copolymer, SRU), 114678-27-2; (1,3-bis(4-aminobenzoyl)-propane)((±)-3-methyladipic acid) (copolymer), 114677-57-5; (1,3-bis(4-aminobenzoyl)propane)((±)-3-methyladipic acid) (copolymer, SRU), 114718-84-2; (1,3-bis(4-aminobenzoyl)-propane)(hydromuconic acid) (copolymer), 114678-50-1; (1,3-bis(4-aminobenzoyl)propane)(hydromyconic acid) (copolymer, SRU), 114718-83-1; (1,3-bis(4-aminobenzoyl)propane)(2,6-naphthalenedicarboxylic acid) (copolymer), 114677-58-6; (1,3-bis(4-aminobenzoyl)propane)(2,6-naphthalenedicarboxylic acid) (copolymer, SRU), 114678-28-3; (1,3-bis(4-aminobenzoyl)-propane)(terephthalic acid) (copolymer), 114677-59-7; (1,3-bis-(4-aminobenzoyl)propane)(terephthalic acid) (copolymer, SRU), 114678-29-4; (1,3-bis(4-aminobenzoyl)propane)(isophthalic acid) (copolymer), 114677-60-0; (1,3-bis(4-aminobenzoyl)propane)-(isophthalic acid) (copolymer, SRU), 114678-30-7; (1,3-bis(4-

aminobenzoyl)propane)(3-methylglutaric acid) (copolymer), 114677-61-1; (1,3-bis(4-aminobenzoyl)propane)(3-methylgutaric acid) (copolymer, SRU), 114678-31-8; (1,3-bis(4-aminobenzoyl)-propane)(2-methylglutaric acid) (copolymer), 114677-62-2; (1,3-bis(4-aminobenzoyl)propane)(2-methylglutaric acid) (copolymer), 114718-89-7; (1,3-bis(4-aminobenzoyl)propane)(2,2-dimethylglutaric acid) (copolymer), 114677-63-3; (1,3-bis(4-aminobenzoyl)propane)(2,2-dimethylglutaric acid) (copolymer, SRU), 114718-85-3; (1,3-bis(4-aminobenzoyl)propane)(3,3-dimethylglutaric acid) (copolymer), 114677-64-4; (1,3-bis(4-aminobenzoyl)propane)(3,3-dimethylglutaric acid) (copolymer, SRU), 114678-32-9; (1,3-bis(4-aminobenzoyl)propane)(diglycolic acid) (copolymer), 114677-65-5; (1,3-bis(4-aminobenzoyl)propane)(diglycolic acid) (copolymer, SRU), 114678-33-0; (1,3-bis(4-aminobenzoyl)propane)(maleic acid) (copolymer), 114677-66-6; (1,3-bis(4-aminobenzoyl)propane)(maleic acid) (copolymer, SRU), 114678-34-1; (1,3-bis(4-aminobenzoyl)propane)(fumaric acid) (copolymer), 114677-67-7; (1,3-bis(4-aminobenzoyl)propane)(fumaric acid) (copolymer, SRU), 114678-35-2; (1,3-bis(4-aminobenzoyl)propane)(pentanedioic acid)(hexanedioic acid) (copolymer), 114677-68-8; (1,3-bis(4-aminobenzoyl)propane)(octanedioic acid)(nonanedioic acid) (copolymer), 114677-69-9; (1,3-bis(4-aminobenzoyl)propane)(nonanedioic acid)(decanedioic acid) (copolymer), 114677-70-2; (1,3-bis(4-aminobenzoyl)-propane)(pentanedioic acid)(nonanedioic acid) (copolymer), 114677-71-3; (1,3-bis(4-aminobenzoyl)propane)(heptanedioic acid)(nonanedioic acid) (copolymer), 114677-72-4; (1,3-bis(4-aminobenzoyl)propane)(decanedioic acid)(hexanedioic acid) (copolymer), 114677-73-5; (1,3-bis(4-aminobenzoyl)propane)(decanedioic acid)(dodecanedioic acid) (copolymer), 114677-74-6; (1,3-bis(4-aminobenzoyl)propane)(1,4-bis(4-aminobenzoyl)butane)(dodecanedioic acid) (copolymer), 114677-75-7; (1,2-bis(4-aminobenzoyl)ethane)(1,4-bis(4-aminobenzoyl)butane)(dodecanedioic acid) (copolymer), 114677-76-8; (1,3-bis(4-aminobenzoyl)propane)(1,4-bis(4-aminobenzoyl)butane)(nonanedioic acid)(dodecanedioic acid) (copolymer), 114677-77-9; (1,2-bis(4-aminobenzoyl)ethane)(1,4-bis(4-aminobenzoyl)butane)(nonanedioic acid)(dodecanedioic acid) (copolymer), 114677-78-0; (bis(4-aminophenoxy)propane)(pentanedioic acid) (copolymer), 114691-72-4; (bis(4-aminophenoxy)propane)(pentanedioic acid) (copolymer, SRU), 114678-36-3; (bis(4-aminophenoxy)-propane)(hexanedioic acid) (copolymer), 114691-73-5; (bis(4-aminophenoxy)propane)(hexanedioic acid) (copolymer, SRU), 114678-37-4; (bis(4-aminophenoxy)propane)(nonanedioic acid) (copolymer), 114691-74-6; (bis(4-aminophenoxy)propane)(nonanedioic acid) (copolymer, SRU), 114678-38-5; (bis(4-aminophenoxy)propane)(decanedioic acid) (copolymer), 114691-75-7; (bis(4-aminophenoxy)propane)(decanedioic acid) (copolymer, SRU), 114678-39-6; (bis(4-aminophenoxy)hexane)(nonanedioic acid) (copolymer), 114691-76-8; (bis(4-aminophenoxy)hexane)-(nonanedioic acid) (copolymer, SRU), 114678-40-9; (bis(4-aminophenoxy)octane)(pentanedioic acid) (copolymer), 114677-79-1; (bis(4-aminophenoxy)octane)(pentanedioic acid) (copolymer, SRU), 114678-41-0; (bis(4-aminophenoxy)octane)(hexanedioic acid) (copolymer), 114691-77-9; (bis(4-aminophenoxy)octane)-(hexanedioic acid) (copolymer, SRU), 114678-42-1; 1,3-propanediyl bis[4-(pentylamido)benzoate], 114678-43-2; 1,3-propanediyl bis-[4-(hexylamido)benzoate], 114678-44-3; 1,3-propanediyl bis[4-(octylamido)benzoate], 114678-45-4; 1,3-propanediyl bis[4-(nonylamido)benzoate], 114691-79-1; 1,3-propanediyl bis[4-(4-pentylbenzamido)benzoate], 114678-46-5; 1,3-propanediyl bis-[4-(4-hexylbenzamido)benzoate], 114678-47-6; 1,3-propanediyl bis[4-(4-heptylbenzamido)benzoate], 114678-48-7; 1,3-propanediyl bis[4-(4-octylbenzamido)benzoate], 114678-49-8.

References and Notes

(1) Morgan, P. W. *Macromolecules* **1977**, *10*, 1381.
(2) Aharoni, S. M. *Macromolecules* **1987**, *20*, 2010.
(3) Jin, J. I.; Antoun, S.; Ober, C.; Lenz, R. W. *Br. Polym. J.* **1980**, *12*, 132.
(4) Aharoni, S. M. *Macromolecules* **1979**, *12*, 94.
(5) Aharoni, S. M. *J. Polym. Sci., Polym. Phys. Ed.* **1980**, *18*, 1303.
(6) Aharoni, S. M. *Macromolecules* **1981**, *14*, 222.
(7) Shmueli, U.; Traub, W.; Rosenheck, K. *J. Polym. Sci., Polym. Phys. Ed.* **1969**, *7*, 515.
(8) Aharoni, S. M. *J. Macromol. Sci.—Phys.* **1982**, *B21*, 105.
(9) Aharoni, S. M. *Mol. Cryst. Liq. Cryst. Lett.* **1980**, *56*, 237.
(10) Aharoni, S. M. *J. Macromol. Sci.—Phys.* **1982**, *B21*, 287.
(11) Aharoni, S. M. *J. Appl. Polym. Sci.* **1980**, *25*, 2891.
(12) Aharoni, S. M. *J. Polym. Sci., Polym. Phys. Ed.* **1981**, *19*, 281.
(13) Aharoni, S. M. *Macromolecules* **1987**, *20*, 877.
(14) Jeffrey, G. A. *Acc. Chem. Res.* **1986**, *19*, 168.
(15) Pfannemüller, B.; Welte, W.; Chin, E.; Goodby, J. W. *Liquid Crystals* **1986**, *1*, 357.
(16) Noël, C. In *Recent Advances in Liquid Crystalline Polymers*; Chapoy, L. L., Ed.; Elsevier Applied Science: London, 1985; pp 135–164.
(17) Kelker, H.; Hatz, R. *Handbook of Liquid Crystals*; Verlag Chemie: Weinheim, 1980; pp 372–383.
(18) Sackmann, H.; Demus, D. *Mol. Cryst. Liq. Cryst.* **1973**, *21*, 239.
(19) Krigbaum, W. R.; Watanabe, J. *Polymer* **1983**, *24*, 1299.
(20) Aharoni, S. M.; Walsh, E. K. *Macromolecules* **1979**, *12*, 271.
(21) Aharoni, S. M. *Polymer* **1980**, *21*, 21.
(22) Strzelecki, L.; Van Luyen, D. *Eur. Polym. J.* **1980**, *16*, 299.
(23) Bartulin, J.; Ramos, M. L.; Rivas, B. L. *Polym. Bull.* **1986**, *15*, 405.
(24) Yamazaki, N.; Matsumoto, M.; Higashi, F. *J. Polym. Sci., Polym. Chem. Ed.* **1975**, *13*, 1373.
(25) Aharoni, S. M.; Hammond, W. B.; Szobota, J. S.; Masilamani, D. *J. Polym. Sci., Polym. Chem. Ed.* **1984**, *22*, 2579.
(26) Laakso, T. M.; Reynolds, D. D. *J. Am. Chem. Soc.* **1960**, *82*, 3640.
(27) Manzini, G.; Crescenzi, V.; Ciana, A.; Ciceri, L.; Della Fortuna, G.; Zotteri, L. *Eur. Polym. J.* **1973**, *9*, 941.
(28) Morgan, P. W. *Condensation Polymers: By Interfacial and Solution Methods*; Interscience: New York, 1965; pp 6–7.
(29) Flory, P. J. *Principles of Polymer Chemistry*; Cornell University Press: Ithaca, NY, 1953; pp 87–91.
(30) Jackson, W. J.; Kuhfuss, H. F. U.S. Patent 4 182 842, 1980.
(31) East, A. J.; Charbonneau, L. F.; Calundann, G. W. U.S. Patent 4 330 457, 1982.
(32) McIntyre, J. E.; Milburn, A. H. U.S. Patent 4 272 625, 1981.
(33) Gopal, J.; Srinivasan, M. *Makromol. Chem.* **1986**, *187*, 1.
(34) Preston, J. U.S. Patent 3 926 923, 1975.
(35) Osman, M. A. *Polymer* **1987**, *28*, 713.
(36) Shashoua, V. E.; Eareckson, W. M. *J. Polym. Sci.* **1959**, *40*, 343.
(37) Farrow, G.; McIntosh, J.; Ward, I. M. *Makromol. Chem.* **1960**, *38*, 147.
(38) Fradet, A.; Heitz, W. *Makromol. Chem.* **1987**, *188*, 1233.
(39) Arnold, H.; Sackmann, H. *Z. Phys. Chem. (Leipzig)* **1960**, *213*, 137, 145.
(40) Volksen, W.; Lyerla, J. R., Jr.; Economy, J.; Dawson, B. *J. Polym. Sci., Polym. Chem. Ed.* **1983**, *21*, 2249.
(41) Meurisse, P.; Noël, C.; Monnerie, L.; Fayolle, B. *Br. Polym. J.* **1981**, *13*, 55.
(42) Noël, C.; Friedrich, C.; Bosio, L.; Strazielle, C. *Polymer* **1984**, *25*, 1281.
(43) Keller, P. *Mol. Cryst. Liq. Cryst.* **1985**, *123*, 247.
(44) Iimura, K.; Koide, N.; Tanabe, H.; Takeda, M. *Makromol. Chem.* **1981**, *182*, 2569.
(45) Iimura, K.; Koide, N.; Ohta, R.; Takeda, M. *Makromol. Chem.* **1981**, *182*, 2563.
(46) Galli, G.; Nieri, P.; Ober, C.; Chiellini, E. *Makromol. Chem., Rapid Commun.* **1982**, *3*, 548.
(47) Galli, G.; Laus, H.; Angeloni, A. S.; Ferruti, P.; Chiellini, E. *Makromol. Chem., Rapid Commun.* **1983**, *4*, 681.
(48) Makaruk, L.; Polanska, H.; Ksiezakowska, E.; Wazynska, B. *Polym. J.* **1985**, *17*, 1055.
(49) Ciferri, A. In *Polymer Liquid Crystals*; Ciferri, A., Krigbaum, W. R., Meyer, R. B., Eds.; Academic: New York, 1982; pp 63–102.
(50) Noël, C. In *Polymeric Liquid Crystals*; Blumstein, A., Ed.; Plenum: New York, 1985; pp 21–63.
(51) Coleman, M. M.; Skrovanek, D. J.; Howe, S. E.; Painter, P. C. *Macromolecules* **1985**, *18*, 301.
(52) Skrovanek, D. J.; Howe, S. E.; Painter, P. C.; Coleman, M. M. *Macromolecules* **1985**, *18*, 1676.
(53) Kyotani, M.; Yoshida, K.; Ogawara, K.; Kanetsuna, H. *J. Polym. Sci., Polym. Phys. Ed.* **1987**, *25*, 501.
(54) Wunderlich, B. *Macromolecular Physics*; Academic: New York, 1973; Vol. 1, pp 131–140.
(55) Itoh, T. *Jpn. J. Appl. Phys.* **1976**, *15*, 2295.
(56) De Vries, A. *Mol. Cryst. Liq. Cryst.* **1985**, *131*, 125.
(57) Chistyakov, I. G. In *Advances in Liquid Crystals*; Brown, G. H., Ed.; Academic: New York, 1975; Vol. 1, pp 143–168.
(58) Leadbetter, A. J.; Norris, E. K. *Mol. Phys.* **1979**, *38*, 669.
(59) Saupe, A. *Mol. Cryst. Liq. Cryst.* **1969**, *7*, 59.
(60) Pape, E. H.; Schröder, K.; Zugenmaier, P. *Mol. Cryst. Liq. Cryst. Lett.* **1987**, *4*, 165.
(61) Bonart, R.; Hosemann, R. *Makromol. Chem.* **1960**, *39*, 105.
(62) Hosemann, R. *Polymer* **1962**, *3*, 349.

(63) Wunderlich, B.; Grebowicz, J. *Adv. Polym. Sci.* **1984**, *60/61*, 1.
(64) Krigbaum, W. R. *J. Appl. Polym. Sci. Appl. Polym. Symp.* **1985**, *41*, 105.
(65) Thomas, E. L.; Wood, B. A. *Faraday Discuss. Chem. Soc.* **1985**, *79*, 229.
(66) Poulin-Dandurand, S.; Perez, S.; Revol, J.-F.; Brisse, F. *Polymer* **1979**, *20*, 419.
(67) Tanford, C. *Physical Chemistry of Macromolecules*; Wiley: New York, 1961; pp 344–346.
(68) Blumstein, A.; Maret, G.; Vilasagar, S. *Macromolecules* **1981**, *14*, 1543.

Block Copolymers Containing Monodisperse Segments Produced by Ring-Opening Metathesis of Cyclic Olefins

Louis F. Cannizzo and Robert H. Grubbs*

Arnold and Mabel Beckman Laboratories of Chemical Synthesis,† California Institute of Technology, Pasadena, California 91125. *Received July 31, 1987*

ABSTRACT: Block copolymers (A–B and A–B–A) containing segments of narrow molecular weight distribution (hereafter designated as monodisperse) were synthesized by ring-opening metathesis polymerization using titanacyclobutane **2** as the catalyst. The monomers polymerized were norbornene, benzonorbornadiene, 6-methylbenzonorbornadiene, and *endo*- and *exo*-dicyclopentadiene with the living polymers produced containing up to 50 monomers in each segment. The living polymers were end capped (by a Wittig-type reaction) with acetone and chromatographed to give samples free of catalyst. Three representative examples are the diblocks **35** and **38** with PDI's (polydispersity indices) of 1.08 and 1.14, respectively, and the triblock **36** with a PDI of 1.14. Analysis by differential scanning calorimetry (DSC) showed a single T_g for the block copolymers of polynorbornene and poly(*exo*-dicyclopentadiene), indicating the two polymers are compatible.

Introduction

The study and utilization of block copolymers (both diblock and triblock) has proceeded rapidly since their initial synthesis in the early 1960s.[1] Key to development of this unique and highly useful class of copolymers is the concurrent discovery of living polymerization systems[2] which produced well-defined monodisperse segments of controlled molecular weight. Ring-opening metathesis polymerization (ROMP) is developing into a method of controlled polymerization comparable to known living anionic, cationic, and group transfer systems. To date, the living polymerization of the cyclic olefin norbornene has been reported for titanium,[3] tantalum,[4] and tungsten[5] metathesis systems (eq 1).

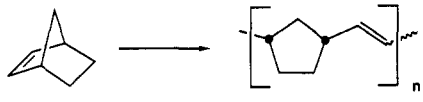

(1)

Our research group has extensively studied the olefin metathesis chemistry of titanacyclobutanes[6] and other catalysts. We have applied this knowledge to organic synthesis[7] and in polymer applications have synthesized end-capped polyalkenamers,[8] conducting[9] and rigid[10] polymers, and chelating polyethers.[11] In further developing titanacyclobutanes as highly versatile metathesis polymerization catalysts we are currently exploring their use in block copolymer synthesis. We have previously reported the blocking of norbornene with 3,4-diisopropylidenecyclobutene to give a conducting polymer with improved mechanical properties compared to the parent cyclobutene polymer.[9a]

In this paper we wish to report the results of our investigations into block copolymer synthesis via titanacyclobutanes.

† Contribution no. 7639.

Results and Discussion

Metathesis Polymerization by Titanacyclobutanes. In order to understand the use of titanacyclobutanes in metathesis polymerization a brief review is needed. Gilliom and Grubbs[3] have demonstrated that metallacycles **1** and **2** (derived from norbornene and 3,3-dimethylcyclopropene, respectively) upon reaction with norbornene (**3**) give monodisperse polynorbornene (**4**) (PDI $\simeq$ 1.1) with virtually no chain transfer or termination. The catalyst is active at higher temperatures (≥65 °C), and upon cooling to room temperature the living polymer is stable for several days. If stored at room temperature under an inert atmosphere this system retains some activity even after several months. Rapid decomposition is observed, however, at the polymerization temperature in the absence of monomer.

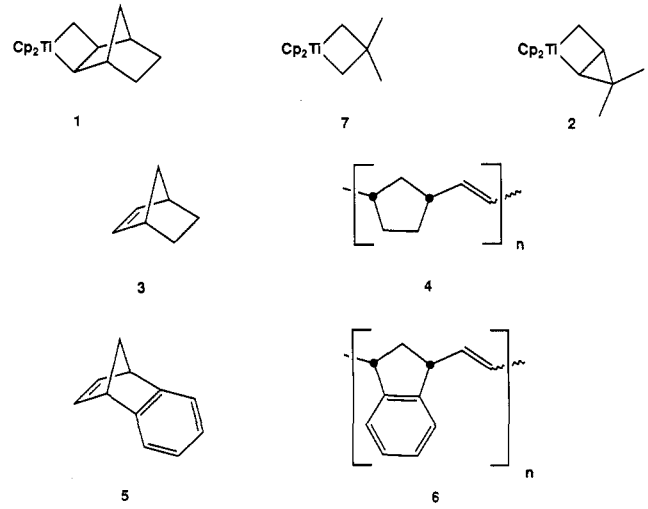

Initial Studies. In order to synthesize block copolymers, it was necessary to find cyclic olefin monomers other than norbornene that titanacyclobutanes would

0024-9297/88/2221-1961$01.50/0